United States
Environmental Protection
Agency

Municipal Environmental Research
Laboratory
Cincinnati OH 45268

EPA-600/2-79-084
August 1979

Research and Development

EPA

Field Testing of Prototype Acoustic Emission Sewer Flowmeter

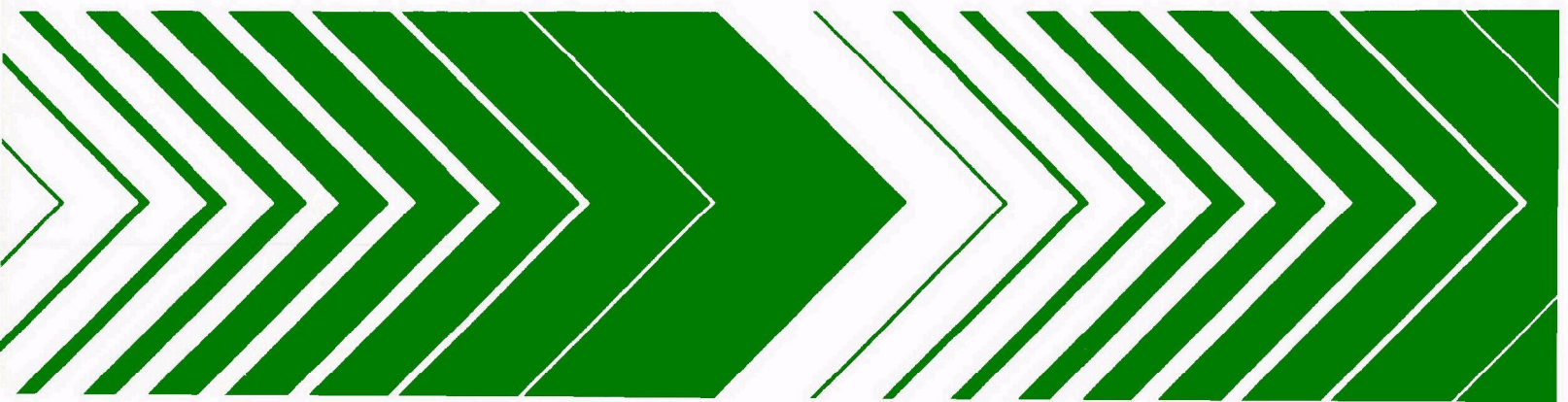

RESEARCH REPORTING SERIES

Research reports of the Office of Research and Development, U.S. Environmental Protection Agency, have been grouped into nine series. These nine broad categories were established to facilitate further development and application of environmental technology. Elimination of traditional grouping was consciously planned to foster technology transfer and a maximum interface in related fields. The nine series are:

1. Environmental Health Effects Research
2. Environmental Protection Technology
3. Ecological Research
4. Environmental Monitoring
5. Socioeconomic Environmental Studies
6. Scientific and Technical Assessment Reports (STAR)
7. Interagency Energy-Environment Research and Development
8. "Special" Reports
9. Miscellaneous Reports

This report has been assigned to the ENVIRONMENTAL PROTECTION TECHNOLOGY series. This series describes research performed to develop and demonstrate instrumentation, equipment, and methodology to repair or prevent environmental degradation from point and non-point sources of pollution. This work provides the new or improved technology required for the control and treatment of pollution sources to meet environmental quality standards.

This document is available to the public through the National Technical Information Service, Springfield, Virginia 22161.

EPA-600/2-79-084
August 1979

FIELD TESTING OF PROTOTYPE ACOUSTIC EMISSION SEWER FLOWMETER

by

K. M. Foreman
Research Department
Grumman Aerospace Corporation
Bethpage, New York 11714

Contract No. 68-03-2525

Project Officer

Hugh Masters
Storm and Combined Sewer Section
Wastewater Research Division
Municipal Environmental Research Laboratory (Cincinnati)
Edison, New Jersey 08817

MUNICIPAL ENVIRONMENTAL RESEARCH LABORATORY
OFFICE OF RESEARCH AND DEVELOPMENT
U.S. ENVIRONMENTAL PROTECTION AGENCY
CINCINNATI, OHIO 45268

DISCLAIMER

This report has been reviewed by the Municipal Environmental Research Laboratory, U.S. Environmental Protection Agency, and approved for publication. Approval does not signify that the contents necessarily reflect the views and policies of the U.S. Environmental Protection Agency, nor does mention of trade names of commercial products constitute endorsement or recommendation for use.

FOREWORD

The Environmental Protection Agency was created because of increasing public and government concern about the dangers of pollution to the health and welfare of the American people. Noxious air, foul water, and spoiled land are tragic testimony to the deterioration of our natural environment. The complexity of the environment and the interplay between its components require a concentrated and integrated attack on the problem.

Research and development is that necessary first step in problem solution and it involves defining the problem, measuring its impact, and searching for solutions. The Municipal Environmental Research Laboratory develops new and improved technology and systems for the prevention, treatment, and management of wastewater and solid and hazardous waste pollutant discharges from municipal and community sources, for the preservation and treatment of public drinking water supplies, and to minimize the adverse economic, social, health, and aesthetic effects of pollution. This publication is one of the products of that research; a most vital communications link between the researcher and the user community.

The need exists to develop innovative, passive, nonintrusive, and low cost solutions to the problems of continuous measurement and recording of flows in storm and combined sewers. This experimental investigation is of one such technique that monitors the pseudosound produced by flow past a channel discontinuity. The results of laboratory and field tests demonstrate the feasibility of this method of flow measurement using an accelerometer transducer attached to the outside surface of a flow channel.

Francis T. Mayo, Director
Municipal Environmental Research
Laboratory

ABSTRACT

This research project was designed to verify the acoustic emission flowmeter concept in the natural operating environment of different storm sewer field sites. The flowmeter is a novel, passive, nonintrusive technique that uses the local sound resulting from partial transformation of the pressure loss of flow at a channel or conduit discontinuity. In this context, a discontinuity is any significant change in channel cross section or flow direction. Other objectives were to examine the feasibility of calibrating flowmeter field installations by means of geometrically similar small scale laboratory models, and to explore the suitability of sewer manholes as flowmeter sensor installation locations.

The three field sites used and the test results correlating acoustic characteristics and physical flow rate of stormwater are described in the body of this report.

The investigation demonstrated that the flowmeter principles hold true in large storm sewers of 60 inch (1.5m) diameter and for flow rates up to about 7500 gpm. The measured sound power, in decibels, is related to mass flow rate to the 1.4 to 1.7 power, depending on channel discontinuity characteristics. A manhole appears suitable for sensor installation. Small scale laboratory models appear to simulate fairly well the sound intensity to flow rate relationship of full scale sites according to theoretical scaling laws. However, the spectral features of the acoustic signature appear in conflict with presently formulated theory; additional research into this anomaly is indicated. Recommendations are offered for future testing and system design activities.

This report was submitted in fulfillment of Contract 68-03-2525 by Grumman Aerospace Corporation under sponsorship of the U.S. Environmental Protection Agency. This report covers the period July 6, 1977 to October 6, 1978, and work was completed as of October 6, 1978.

TABLE OF CONTENTS

FIGURES

FIGURES (Continued)

FIGURES (Continued)

ACKNOWLEDGMENT

We acknowledge the assistance of Messrs. Arthur Speidel, Noe Arcas, and Richard Yoos of Grumman Aerospace Corporation (GAC) in conducting the test program and processing the test data.

We are also indebted to Mr. Hugh Masters and Mr. Richard Field of EPA, who provided helpful guidance in keeping the project in correct perspective.

SECTION 1
INTRODUCTION

The investigations and results described in this final technical report for EPA Contract 68-03-2525 concern a novel, passive, nonintrusive, sewer flowmeter approach called the acoustic emission flowmeter (U.S. Patent 3,958,458, May 25, 1976). This kind of new technology is needed to solve the urgent problems of measurement and recording of storm and combined sewer flows for management, preservation, and treatment of national water resources. With the documentation presented in this report, the technical and operational base of data has been vastly expanded, thereby enhancing the credibility of a highly unconventional and innovative flowmeter concept.

The acoustic emission flowmeter utilizes the local, nonpropagating sound resulting from the partial transformation of flow pressure loss at a discontinuity in a channel or conduit. Earlier work, principally in the research laboratory (Ref. 1) demonstrated the basic mechanism of the flowmeter concept for a large variety of open and closed channel flows and channel materials representative of actual sewer networks. However, the much reduced geometric size and flow quantity imposed by laboratory conditions provided uncertainty about the extrapolation to more realistic full scale field conditions of physical size, quantity, and flow quality. Somewhat mitigating these doubts were the confirmatory indications of a very limited preview field test involving monitoring sanitary sewage flow entering an industrial waste treatment plant.

The present investigation has been geared principally to seeking verification of the earlier examinations, but in the natural environment of three different storm sewer field sites. The geometric scale of the new flow channel is twenty times the laboratory scale, and the maximum storm sewer flows are almost two orders of magnitude larger than the greatest laboratory flow. Other objectives of the current work have been a) to examine the feasibility of calibrating field installations of the flowmeter

system by means of geometrically similar, small scale models in the convenience of the laboratory environment, and b) to explore the suitability of using sewer manholes as sensor installation locations. The passive sensor used in the acoustic emission flowmeter is an accelerometer, and its attachment to the nonwetted surfaces of the conduit is through the intermediary of a dedicated mounting stud cemented to the channel wall.

The principal investigator has endeavored also to address problems of future implementation of the technique, during the present research phase. Several alternative adhesives and mounting stud installation procedures have been evaluated under conditions of long term natural environmental exposure. During the last quarter of the test program, a portable, simplified, real time, sound monitor system also was used concurrent with the more usual procedure of recording sound data and transferring the taped sound to a Fourier Analyzer at a later time for spectral distribution processing; comparative results are given here.

The body of this report describes the three field sites and the test results of acoustic emission and physical flow rate. Measurements were made in the field and for one-twentieth scale, geometrically similar, laboratory models. Conclusions of the investigation and recommendations for future action directly follow this introductory section.

SECTION 2
CONCLUSIONS

Field investigations, involving unprecedented stormwater flow rates and storm sewer sizes, have verified the operational principles of the acoustic emission flowmeter in real working environments. Using a prototype flowmeter system, acoustic measurements were made at three different sites of dry weather and stormwater flow rates up to about 7500 gpm over a 10-month test period. Small acoustic sensor mounts installed on weathered concrete surfaces remained operationally intact and secure at normally unprotected public works sites during this period.

Unambiguous acoustic signals have been correlated with physically measured flow rates at these three different field sites. Sound power has been found to be related to flow rate to the 1.4 to 1.7 power, depending on the channel discontinuity geometry. This is equivalent to an increase of average sound level intensity of 4 to 5 decibels for each doubling of flow rate. The suitability of low cost, rugged and small accelerometers has been confirmed for monitoring in adverse working environments, including a manhole installation, the dipole-like acoustic radiation caused by flow near a channel discontinuity.

The successful demonstration of principles and extension of operations to realistic full scale field conditions has enhanced the credibility of the innovative and unconventional acoustic emission flowmeter concept.

Precalibration of field installations by using inexpensive, geometrically similar, small scale laboratory models and theoretical scaling laws has been partially demonstrated. The laboratory flow model simulates fairly well the relationship of acoustic emission intensity to flow rate of the full scale field site. However, the sound frequency band in which the modeling agreement was achieved appears at variance with current predictive theory. Without further research this problem could impede a

full understanding of the process and could pose a potential barrier to future implementation without in situ calibrations.

Measurements made with a breadboard, real time, portable acoustic emission monitoring system compared generally favorably with data recorded by the prototype system and processed through a high resolution Fourier Analyzer. This encouraging experience with a quasi-commercial system also provided guidance for signal filtering specifications of an eventual operational flowmeter system.

SECTION 3

RECOMMENDATIONS

The storm sewer demonstration testing reported here has furthered the attractiveness of the passive acoustic emission flowmeter concept for municipal and regional sewer systems. Some basic studies still appear desirable to trace the conversion of flow energy into a spectral distribution of sound intensity for different channel disturbances. This information is particularly needed to characterize better the frequency of expected maximum acoustic intensity and usable harmonics. The prevailing consensus toward combined sewer systems because of economics, suggests that further field examination of the acoustic emission flowmeter should be directed to that application. Finally, it is becoming evident that efficient narrow band signal filtering is needed, particularly above 2000 Hz, to make a real time flowmeter system compatible with the likely spectral quality of accelerometer sensor output for real installations.

Therefore, we recommend the following three step activity as the next phase in the flowmeter development cycle.

- Conduct field tests of the prototype acoustic emission flowmeter system at a well-instrumented combined (sanitary plus stormwater flow) sewer facility. Independent flow rate and flow quality instrumentation should be available at the facility and testing should be conducted at a suitable channel discontinuity for a sufficient time (e.g., months) to experience a wide variety of flow conditions
- Conduct further laboratory and field testing with sufficient fluid dynamics and acoustics measurements to resolve anomalies of acoustic emission characteristic frequency described in the current test phase. Examine possible structural resonance excitation of sensor installations

and response characteristics for at least three different accelerometer designs. Develop theory modifications to reflect empirical results

- Design a prototype flow measurement system combining elements of a portable direct readout, real time sound meter and a narrow band filter circuit compatible with signal outputs of commercially available low cost accelerometer sensors. Purchase components and construct a portable system and conduct shakedown tests at an instrumented field site. After these initial preliminary checkouts, install system at the field site for long term evaluation of performance and reliability relative to EPA objectives.

SECTION 4
SCOPE OF WORK

The primary objective of this project has been to verify the novel acoustic emission flowmeter technique in real field installations. However, it is perceived that the operational utility of the flowmeter would be enhanced if in situ calibration of each installation were unnecessary, and if the ubiquitous sewer manhole could be used for flow sensor locations. The basic theory of the acoustic emission flowmeter requires the empirical determination of a flow calibration parameter associated with the characterizing dimensions of the candidate channel discontinuity.

Our initial approach to preclude full field calibrations has been to employ geometric similarity principles to justify using small scale models for each candidate sewer configuration to be instrumented. Thus, with the convenience and in the controlled conditions of the laboratory, low cost modeling holds the promise of a technically acceptable and economically viable alternative to direct field calibrations. For this reason, the test project has consisted of two phases; one, involving measurements of acoustic emission and associated flow rates entirely in a field environment, and a second phase conducted with one-twentieth scale models of the field sites, in the Grumman Research Laboratory. Data of the latter phase then can be compared to field results and our similarity law hypothesis tested.

Also within the scope of this project has been an exploration of the suitability of sewer manholes for sensor installation.

FIELD TEST PHASE

Three field test sites were selected, at the contract's initiation, with the concurrence of the EPA Technical Monitor. All were within Nassau County, New York, which allowed us to minimize travel distance from the Grumman main facility in Bethpage, New York. The two general areas, Cutter Mill Drain, on the north shore and Baldwin Creek on the south side of Long

Island, previously had been instrumented each with a recording Parshall flume by Department of Agriculture (DoA) Project 208 personnel. Because of several coordination talks with cognizant DoA engineers it had been assumed during precontract negotiations with the EPA that the Project 208 flow measurement equipment would remain in place and be available for this effort; however, the flumes were removed by DoA personnel at an indeterminate time prior to our actual contract award. Therefore, we proposed, as an alternative, physically to measure the flow rate at our test sites by a velocity traverse-integration method. With the EPA Technical Monitor's concurrence, a Marsh McBirney Model 201 flow velocity measurement system was purchased, and a probe support-manual traversing mechanism was constructed for attachment at each test site. A V-notch wier also was used particularly for very low, dry weather flows.

Cutter Mill Drain Site

The Cutter Mill field test location is an historic natural stream in the University Gardens section of the Lake Success area of northwestern Nassau County, New York. The storm drainage area encompasses 260 acres consisting of high value suburban developments (59% area), golf courses (35% area), and major arterial roads (6% area). Dry weather flow is small but continuous and originates from the spilloff of Lake Success which is at about 70 feet (21 m) higher elevation.

The focus of our measurements in this area involved two sites at an open channel conducting the flow away from a 60-inch (1.52 m) diameter underground, reinforced concrete, sewer pipe exiting at a concrete headwall just north of Sussex Road. The open drain continues north for about 530 feet (162 m) before changing into a man-made culvert beneath North Hempstead Turnpike (Northern Boulevard). A reinforced concrete check dam intercepts the drainage ditch about 195 feet (59 m) downstream of the headwall. Both locations, the headwall and check dam, provide well defined but different type discontinuities in the channel that lend themselves to sensor installation for the acoustic emission flowmeter. The flow quantity measured at the headwall is, for practical purposes, the same as that flowing over the checkdam because additional runoff is very small from the surrounding grounds between the two sites.

The 7 foot wide by 7 foot high (2.1 x 2.1 m) headwall location is a sudden enlargement type channel discontinuity for the 60-inch (1.5 m) diameter storm sewer line. Sloping wing walls, made of reinforced concrete, expand the channel to a full 14 foot (4.2 m) width downstream of the headwall, and a concrete apron runout section of about 50 feet (15.2 m) length maintains a uniform and flat drainage bed. At the sewer pipe centerline, there is a step of 0.9 feet (0.27 m) between the bottom of the sewer pipe and the concrete apron. As is evident from Fig 1, the 5 foot (1.5 m) wide paved sloping sides downstream of the wing walls are partially covered by a carpet of grass, weeds, and soil from the adjoining grounds. Thirty feet upstream of the headwall is a manhole where an underground 24-inch (0.61 m) diameter sewer line connects orthogonal to the underground 60-inch (1.5 m) pipeline. The smaller pipe conducts storm water from two curbside catch basins at a naturally low (dip) point of Sussex Road.

Sensor mounting studs were cemented to the sewer pipe roof (at centerline), the headwall, and to the wing walls. The velocity traversing equipment was mounted to the 1 foot (0.3 m) wide top of the concrete headwall.

The reinforced concrete check dam creates an upstream waterpool about 2.7 feet (0.82 m) deep and a downstream free water fall height of about 2 feet (0.61 m). A 6.5 foot (2 m) wide reinforced concerete apron provides a spillway over the dam and the overflow falls into a downstream pool of varying depth caused by a severely eroded drainage bed and the remains of a concrete pavement. As shown by Figs. 1 and 2, the sloping banks of the channel downstream of the check dam are paved with concrete to form two 20 foot (6.1 m) long strips, each 5 feet (1.5 m) wide, paralleling the stream. This check dam provides a second type of channel discontinuity. Sensor mounting studs were cemented to the downstream face of the dam, to the unwetted sloping flanks of the spillway, and to the paved bank of the drain channel downstream of the check dam.

Baldwin Creek Site

The Baldwin Creek study site is located in the community of Baldwin in south central Nassau County, New York. The open channel conveys the effluent of a 60 inch (1.5 m) diameter submerged reinforced concrete storm sewer for

Figure 1. Photo views of the Cutter Mill Drain field test sites, Lake Succes Area, N. Y.

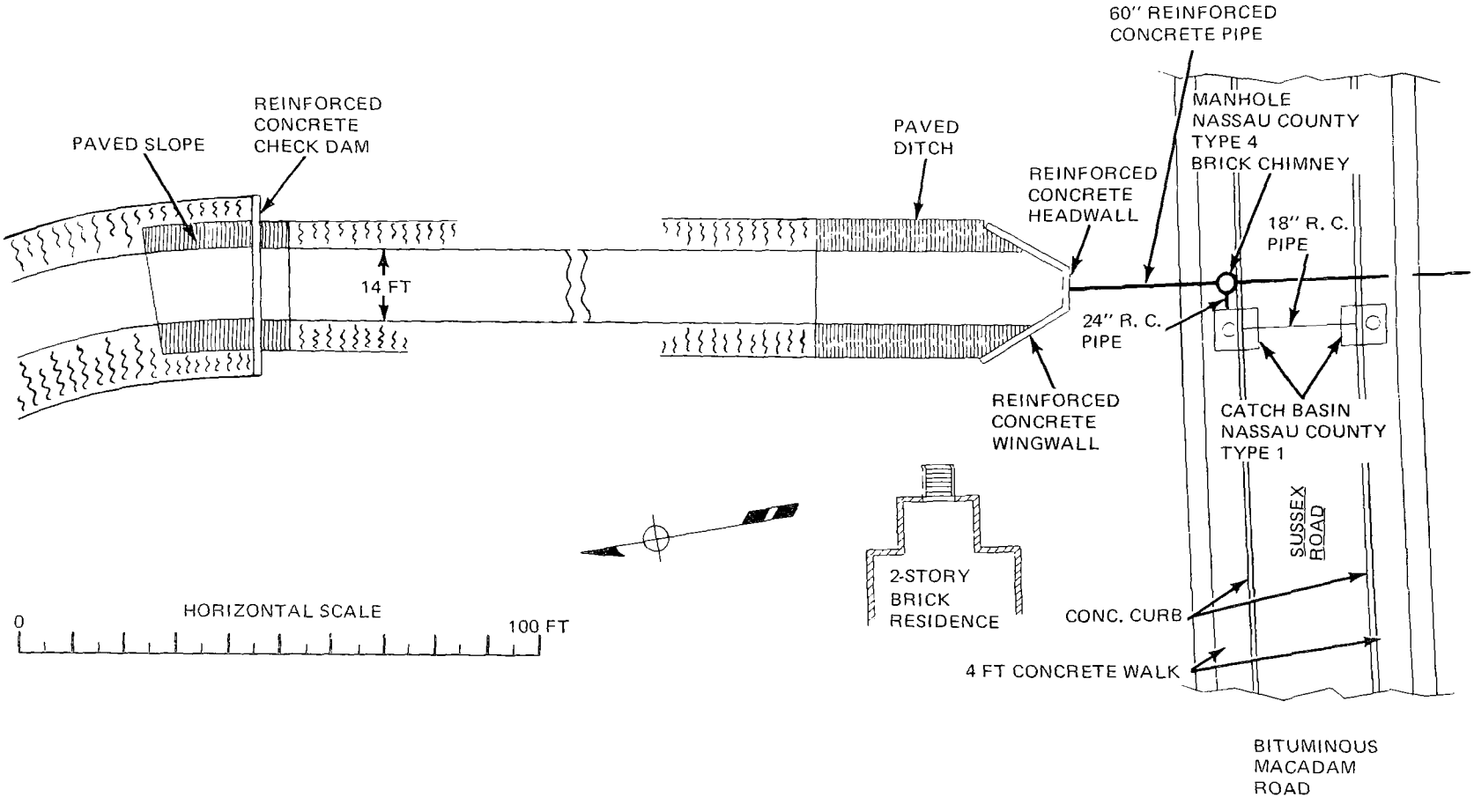

Figure 2. Plan view map of Cutter Mill Drain field test sites. Lake Success area, N.Y.

about 500 feet (150 m) before re-entering a submerged 60 inch (1.5 m) diameter sewer pipe which conducts the flow southward into Parsonage Cove of Hempstead Bay. The open channel is a public works improvement of an originally meandering natural stream through a lowlands swamp area.

The underground storm sewer runs south beneath a public street, Howard Place, (see Fig. 3) before taking a 90 degree eastward turn, runs 60 feet (18.3 m) beneath a grassy land parcel owned by the county, and then takes a 100 degree turn southward, and emerges at a reinforced concrete headwall. Immediately downstream of the headwall is a 20 foot (6.1 m) long concrete channel bed which forms a stepless transition with the bottom of the D-shaped flow channel of the 100 degree turn. This turn is of reinforced concrete construction with a rectangular roof shape and includes a manhole midway through the turn and above the outer radius wall. The 90 degree turn further upstream, is also of reinforced concrete construction and has a manhole rising above the mid-turn position. The sloping banks of the open channel are paved with concrete, to a width of about 10 feet (3. m) as shown by Fig. 4.

The double turn configuration of the submerged sewer offers a third channel discontinuity type to be studied. Sensor mounting studs were cemented to the concrete headwall, at various places along the lower part of the internal surface of the 100 degree turn, at various places along the inner surface of the manhole, and at the inner surface of the junction between the 60 inch diameter pipe and the 100 degree turn.

The Baldwin Creek channel drains storm waters from about 430 acres of an area consisting mainly of single family residential buildings. About 10 acres of two-story apartment dwellings and 40 acres of commercial structures are included in this drainage basin, primarily along two major thoroughfares, Grand Avenue and Woodside Avenue.

Dry weather flow is so slight as to be practically unmeasurable; however, there are retained water pools in the silted creek bed downstream of the headwall, and some trickle movement is visually evident. There is a maximum elevation differential of 25 feet (7.6 m) between the headwater of the Grand Avenue storm sewer feed branch and the open channel culvert, and a

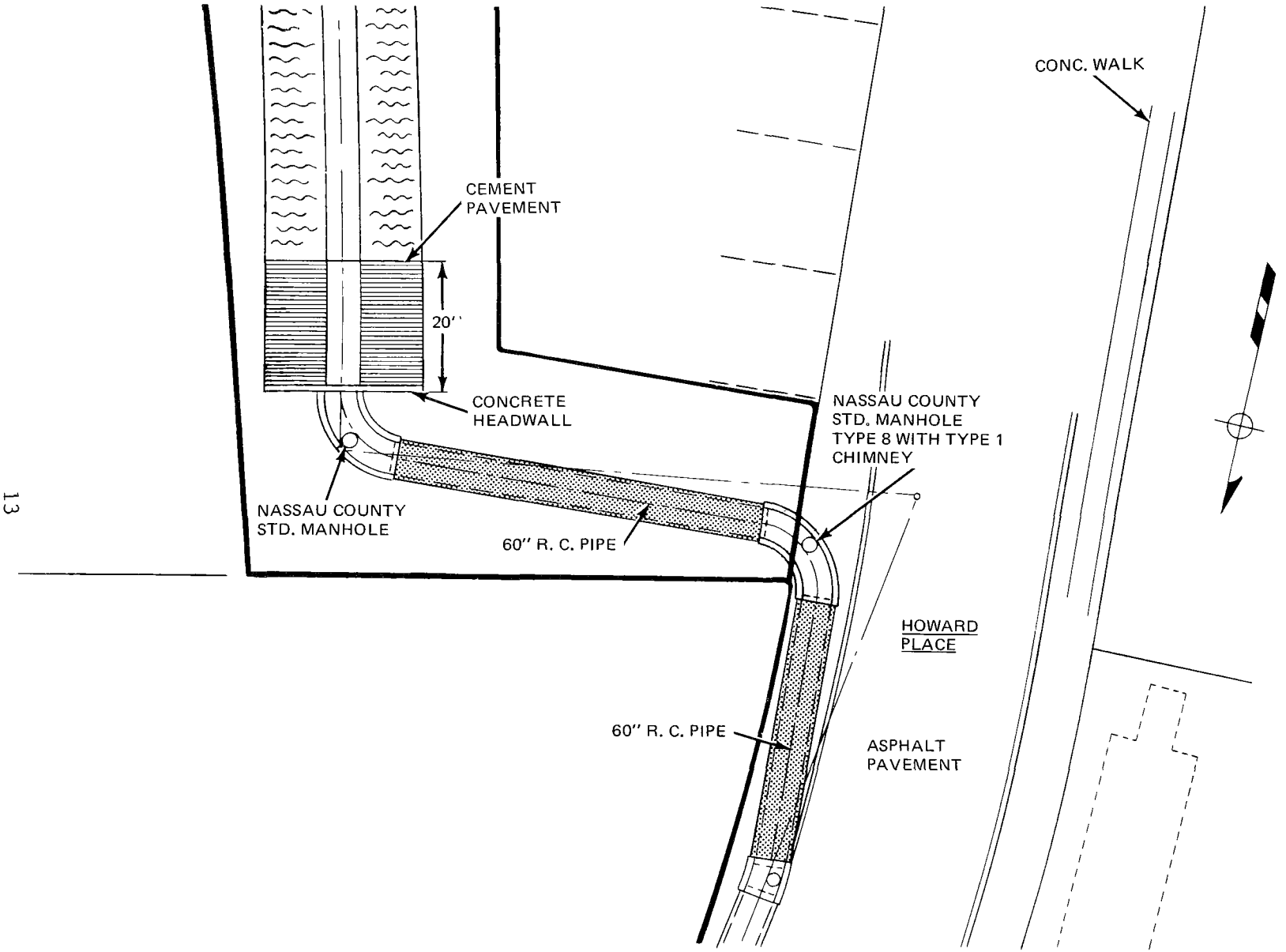

Figure 3. Map of Baldwin Creek field test site, Baldwin, N. Y.

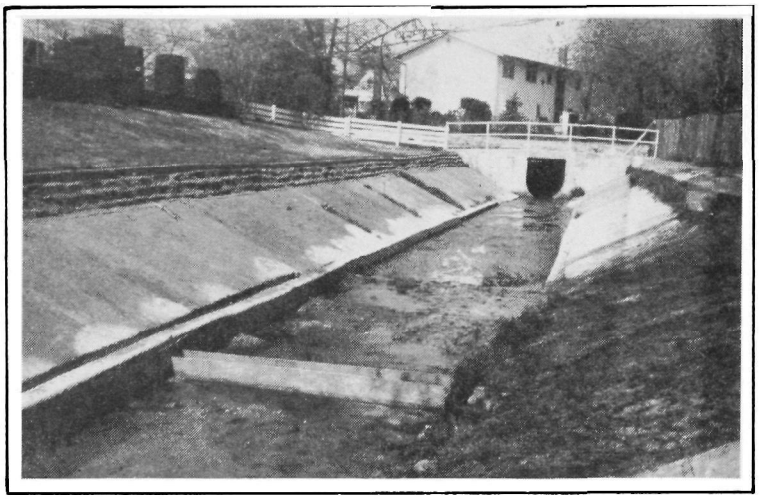

GENERAL AREA VIEW

TOP SURFACE OF 100 DEGREE TURN
SECTION SHOWING MANHOLE COVER

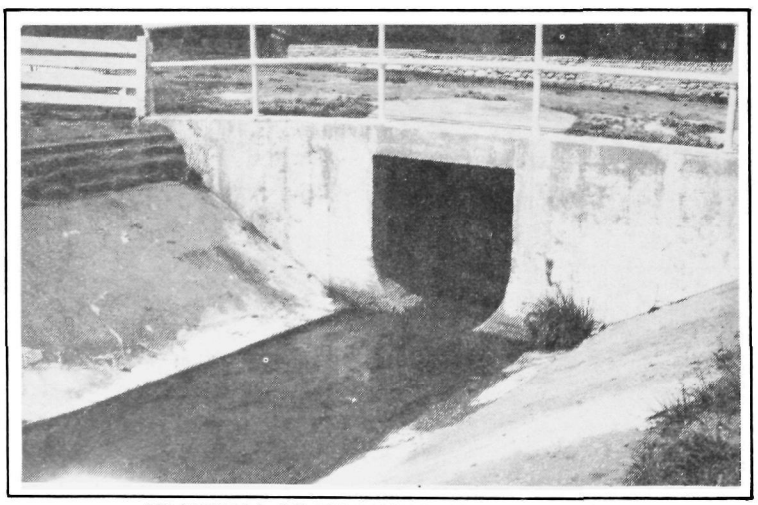

HEADWALL OF 100 DEGREE TURN SECTION

Figure 4. Photo views of Baldwin Creek field test site, Baldwin, N. Y.

maximum of 15 feet (4.6 m) head differential between the beginning of the Woodside Avenue storm sewer branch and the entrance to the open channel. Historic records credit the Baldwin Creek channel with a maximum storm flow rate of about 60,000 gpm (225 m^3/min), or over 8300 pounds per second.

LABORATORY TEST PHASE

In support of the field investigations, models were constructed with the essential geometric features of the three field sites. The water was supplied from the same water flow research facility (see Fig. 5) used in the prior project (Ref. 1). It consists of a 240 gallon (908 m) cylindrical tank, which can be pressurized by a regulated air supply, and a manually controlled flow valve upstream of a 20 feet (6.1 m) length of 3 inch (7.6 cm) diameter steep pipe. This long pipe was taken to simulate the 60 inch (1.5 m) diameter storm sewer pipe at the two field sites, and established the 1/20th scaling size employed for the models. Construction of the models was of a vinyl-mix cement to permit thin sections and with five-mesh (per inch) stainless steel screen reinforcement to simulate the steel reinforcing rods of the actual installations. Molds of wood or aluminum were used to retain the wet cement until hardening. The three-inch diameter water supply pipe was attached by a clamped flange with gasketing to preclude leakage. The entire assembly was supported in a wooden box which was mounted on rails at the facility as shown, typically, by Fig. 6 for the Cutter Mill Drain test site model. In similar manner, as shown by Fig. 7, the 100 degree turn portion of the Baldwin Creek test site, was reproduced in a 1/20th goemetric scale version. Because of the space limitations in the laboratory, the Cutter Mill check dam model was only about 3 feet (0.9 m) downstream from the headwall model instead of a more accurately scaled 10 foot (3.0 m) distance. It was believed that the possible local sound distortion at either discontinuity caused by flow interaction at the other channel change could be discounted in the laboratory environment. Also, because of the small test equipment size the maximum flow rate that could be retained in the model open channel was just under 4.5 lb/sec (2.0 l/sec). To maintain this flow the upstream control valve had to reduce the pressure head in the 3 inch (7.6 cm) line to a value much below the usual tank

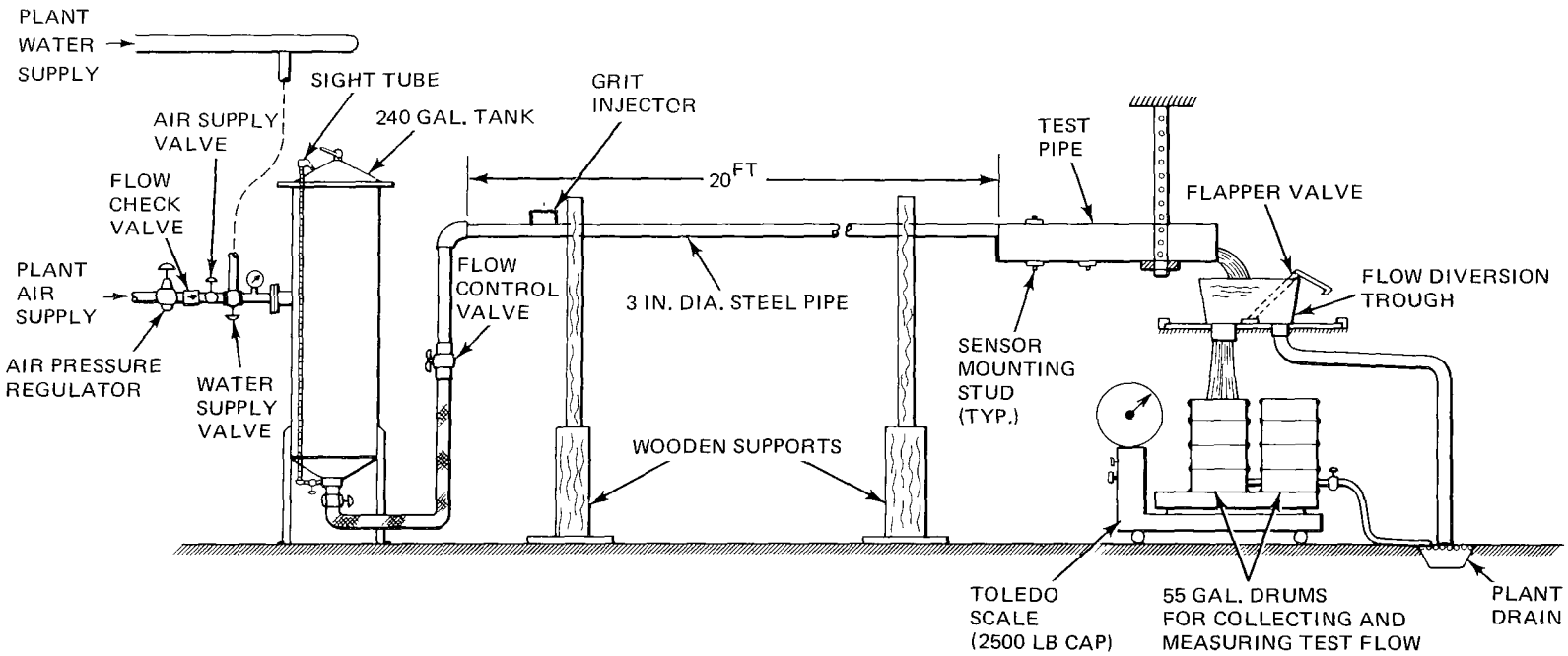

Figure 5. Grumman Reserch water supply facility.

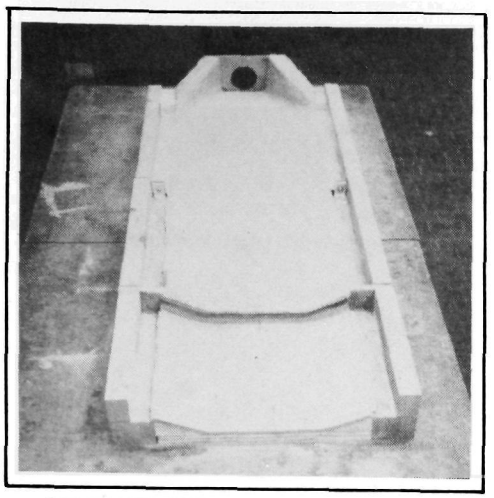

COMBINED MODELS AS FABRICATED

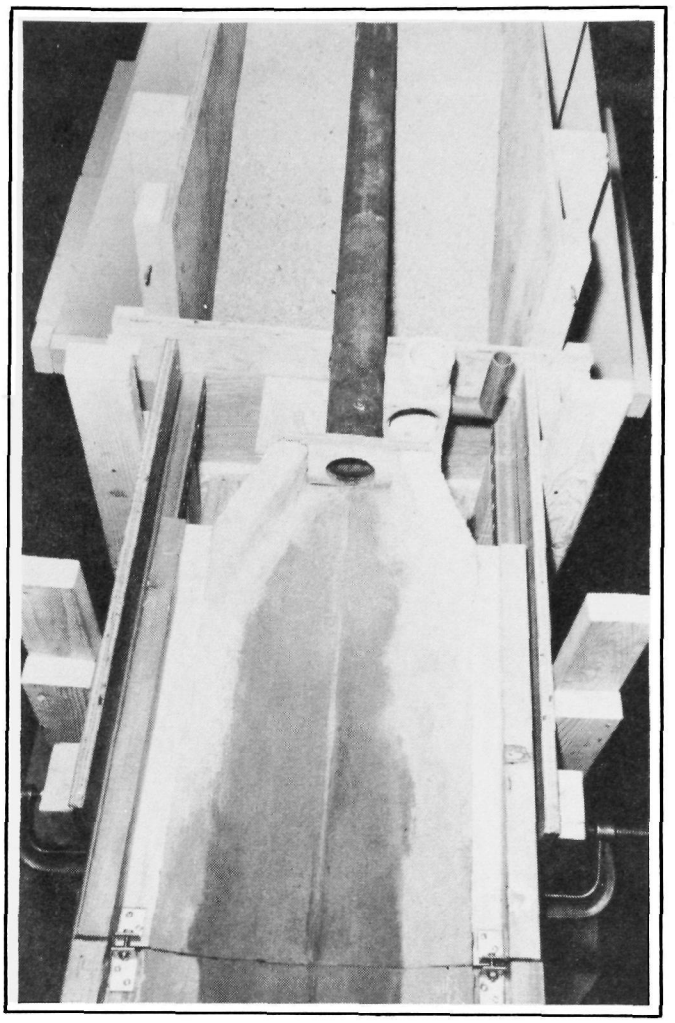

MODEL INSTALLED IN RESEARCH FACILITY

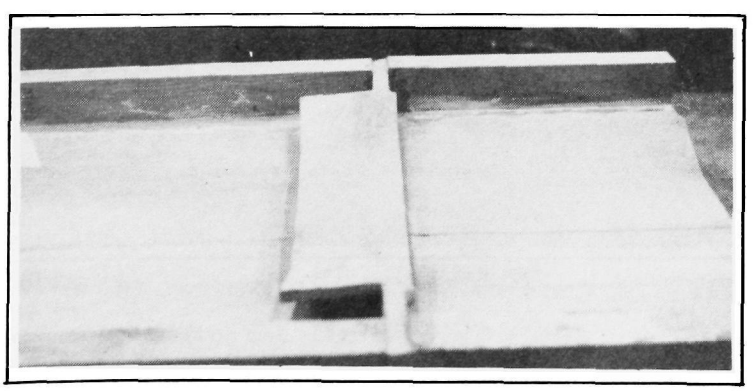

DETAIL OF CHECK DAM MODEL

Figure 6. 1/20th scale model of the Cutter Mill Drain field test sites.

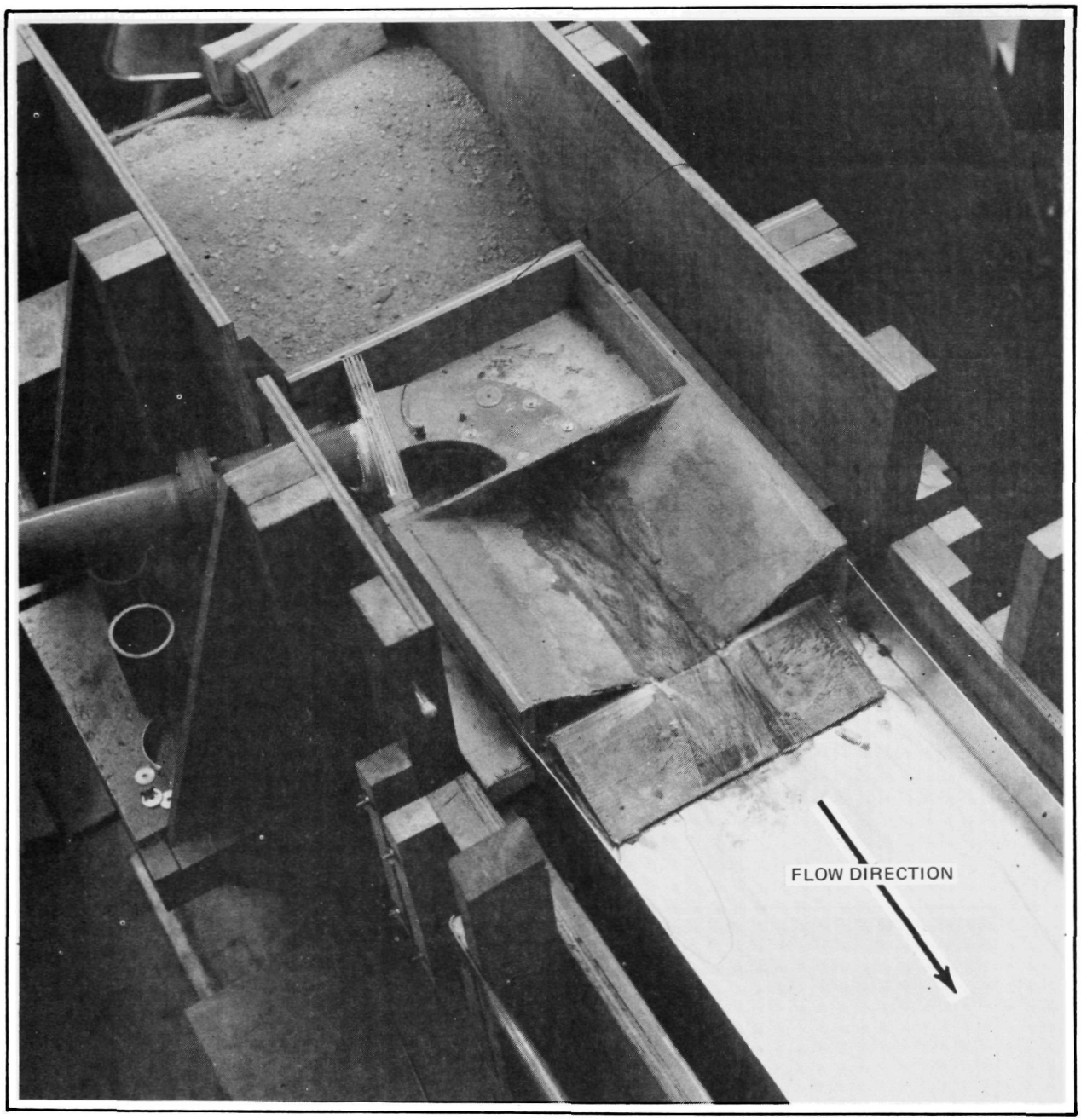

Figure 7. 1/20th scale model of the Baldwin Creek field test site installed in the research facility.

pressure level of about 10-15 psi (69 - 103 kPa). Therefore, the specific energy of the field site open channel flow was not rigorously simulated in the laboratory.

Another imprecise scaling aspect was the large size of the sensor relative to the model's dimensions compared to the field test geometry instrumentation. Thus, each sensor on the model intercepted and was excited by a greater relative portion of the flow's acoustic emission field than in the full scale field installation.

As in the prior project, average flow rate was determined by timing a measured collected weight of water (see Ref. 1); the flow rate usually was averaged over a 20 second interval. Sound recordings were made during the timed interval.

THEORY

Almost every real sewer flow line has turns, steps, junctions of two or more unequal sized lines, and flow control equipment that introduce discontinuities in the channel. In the near field of each discontinuity, the adjustment of the flow to new downstream conditions produces local pressure pulsations and flow unsteadiness. In many cases the periodicity of the pressure pulses is large enough to create audible sound. But the propagation of these pulsations depends on the local mean directed flow velocity rather than the fluid sonic speed. Therefore, this sound predominates only near its source and becomes attenuated with distance from the discontinuity. The near field, nonpropagating sound emitted by the flow is called pseudosound (Refs. 2 and 3). The acoustic emission can be detected by appropriate sensors, such as accelerometers, at the channel boundaries of the flow because the pseudosound radiates as a dipole source, orthogonal to the fluid flow direction. Eventually, the unsteadiness created at the discontinuity becomes dissipated in the complex downstream flow field and becomes coupled to the fluid's far field acoustic radiation pattern.

Sound pressure of pseudosound, p_p, is of the order of ρu^2, where ρ is the average fluid density and u is the average fluid velocity. The dipole source has a total sound power, SP_T, in a free field of

$$SP_T \simeq \frac{P_p^2}{\rho c} \ell^2 \quad (1)$$

where ℓ is the characteristic dimension of the flow channel discontinuity, and c is the fluid sonic speed. Substituting for sound pressure

$$SP_T \simeq \frac{\rho \ell^2 u^4}{c} \quad (2)$$

and Eq. (2) becomes the theoretical basis for the ideal fourth power dependence of sound emission on flow rate. For a particular channel geometry, the volumetric flow rate, Q, is proportional to velocity, so

$$SP_T \simeq Q^4 \quad (3)$$

In the pseudosound process, the direct link to the channel discontinuity is discerned by the sound at a characteristic frequency, f_c, where

$$f_c \simeq c/\delta \quad (4)$$

and δ is the physical dimension characterizing the discontinuity. By analogy to the fundamental physical definition $f = c/\lambda$, where λ is the wavelength of sound, δ can be equated to the wavelength of the characteristic frequency in the fluid. Thus, the physical geometry of the discontinuity provides a guide to determining the characteristic frequency and harmonics where flow-related sound emission can be monitored.

Where the shape of the discontinuity shadows the sound from being radiated the net radiated power is diminished by a factor, ε. For bends and branch junctions, ε tends to unity. For valves and metering sections, values of ε are less than one and must be determined empirically. Furthermore, for sensors mounted to the outer surface of the conduit, there is a sound power loss through the conduit walls, thus transmission coefficient, τ, is approximately proportional to the ratio of channel hydraulic radius to wall thickness, R/t. In cylindrical channels, such as sewer pipes, $\tau \sim D/t$, for source excitation wavelengths larger than $\pi D = \lambda_r$. Loss factors for noncylindrical channels and at frequencies less than λ_r are discussed in Ref. 4. The acoustic coupling of sound from one media to another involves

the acoustic impedance, r = ρc/s, in the two media, where s = the interface surface area.

The acoustic coupling between water and concrete or iron surfaces is about 53 and 15%, respectively (Ref. 1). The poor acoustic coupling of water to air (about 10^{-3}%) predicts that the airborne sound from the flow process at the discontinuity theoretically is an insignificant mechanism compared to the direct coupling of the sound created in the flow with the solid boundaries of the flow channel.

Since the total sound power at the emitting source is of a finite amount per unit time, the further the sound is monitored from the source, the less the sound intensity in each unit area being monitored. However, the integrated sound intensity over the entire radiating surface (at a given distance from the source) never exceeds the total sound power of the source itself plus the zero flow background noise. Total sound power equals intensity times radiating surface area.

SCALING LAWS

The mean square pressure of sound at the inner boundary of a flow channel is

$$\bar{p}^2 = \int_o^\infty F_1(n)\, dn \tag{5}$$

where $F_1(n)$ represents the spectral intensity distribution of the pressure fluctuations in the fluid, for n frequencies.

The pressure variations associated with pseudosound result from velocity fluctuations, du, of the directed pipe flow, U_o. The pressure changes, dp, equal (ρdu) (du) and are proportional to the dynamic pressure ρU_o^2. Then the mean square pressure:

$$\bar{p}^2 \propto \rho^2 U_o^4 \tag{6}$$

The spectral distribution can now be written as

$$\bar{p}^2 = \rho^2 U_o^4 \int_o^\infty \phi_1\left(\frac{n}{n_o}\right) d\left(\frac{n}{n_o}\right) \tag{7}$$

where $\phi_1(n/n_o)$ is an empirical function that must be determined for a range of frequencies relative to the frequency, $n_o \propto c/d$ where d is the depth of flow in an open channel, or the pipe diameter of a continuous, full flowing, cylindrical line.

Using Eqs. (5) and (7) gives

$$\phi_1(n/n_o) = \phi_1(n/U_o/d)$$
$$\phi_1(n/n_o) = \left(\frac{F_1(n)}{\rho^2 U_o^4}\right)(c/d) \tag{8}$$

The elastic properties and constraints of the channel wall material attenuates the fluid pressure variations in a frequency dependent way, T(n), such that the spectral density at the outer surface of the channel structure is

$$F_2(n) = T(n)\ F_1(n) = (n_o/n_1)\phi_2(n/n_o)\ F_1(n)$$

then

$$\bar{p}^2 = \int_o^\infty F_2(n)dn = \rho^2 U_o^4 \int_o^\infty (n_o/n_1)\phi_2(n/n_o)\phi_1(n/n_o)d(n/n_o) \tag{9}$$

where $n_1 = c_m/d_1$; c_m is the sonic speed of the channel wall material and d_1 is the ringing diameter of the pipe (nominally the same as the average pipe diameter for relatively thin-walled cylindrical pipes).

Also,

$$F_2(n) = \rho^2 U_o^4 (n_o/n_1)\phi_3(n/n_o) \tag{10}$$

where $\phi_3(n/n_o)$ is an empirically determined factor that combines the sound source radiating, and wall transmitting, dependencies on sound frequency.

For constant density of the fluid

$$F_2(n) \propto \frac{n_o U_o^4}{n_1}\ \phi_3\ (n/n_o) = U_o^4 \frac{d_1}{c_m}\ \frac{c}{d}\ \phi_3(n/n_o) \tag{11}$$

and

$$\bar{p}^2 \propto \frac{U_o^4 n_o}{n_1} \int \phi_3(n/n_o)\, d(n/n_o) \tag{12}$$

For a flow channel discontinuity characterized by a dimension, h, we can now define a pseudosound characteristic frequency as $n_c = Uc/h$ and the spectral distribution function of intensity takes on a value $F(n_c)$. From Eq. (11)

$$\frac{F_2(n_c)}{U_o^4} = (n_o/n_1)\ \phi_3\ (n_c/n_o)$$

$$\propto (c/c_m)\ (d_1/d)\ \left(\frac{U_c/h}{c/d}\right)$$

Therefore, for geometrically scaled pipelines, if the same pipeline construction material and fluid velocity is used, at the pseudosound characteristic frequency the intensity function is

$$\frac{F_2(n_c)}{U_o^4} \propto \frac{d_1}{h} \tag{13}$$

while at other frequencies

$$\frac{F_2(n)}{U_o^4} \propto d_1\ \phi_3(n/n_o) \tag{13a}$$

Equation (13) is the theory that guides the promotion of small scale geometrically similar models for calibrating full size field installations.

For model flow velocities that duplicate the mean full scale field velocity, the pseudosound intensity for the model should be the same as the geometrically similar field installation. On the other hand, model flow speeds that are lower (e.g., 1/2 to 1/5) than the mean real flow case should result in much lower intensity signals (e.g., by 10 to 30 dB lower) even with otherwise geometric similarity. However, channel dissipative

mechanisms downstream of the discontinuity modify the theoretical fourth power variation of sound intensity with flow velocity; our experience reported here indicates a velocity exponent more in the nature of between 1 and 2, over a broad flow range. The sound intensity signal of the model than should be only about 3 to 15 dB lower than the full scale installation for model flow velocities of 1/2 to 1/5 of the original.

With full geometric similarity and fully duplicated mean flow velocities, the model's quantitative flow rate should be approximately proportional to the square of the linear scaling factor compared to full scale conditions when the sound intensities from the model and full scale channel setups are equal.

SECTION 5

EXPERIMENTAL EQUIPMENT

ACOUSTIC MEASUREMENTS

Two approaches were used in processing the acoustic emission of the flow in this project. The initial method used essentially the same laboratory prototype measurement system previously employed in Ref. 1. This system records signals from an accelerometer sensor mounted to the conduit walls at normally unwetted areas. The tape recorded data are processed through a Fourier Analyzer computer (HP-5465A) at some later date and the spectral distribution of sound intensity is plotted for correlation with physical flow measurements.

The second system also accepts the accelerometer output signal but provides a real time display of sound level amplitude for a particular frequency band. A General Radio (GR) Model 1933 Sound Level Analyzer Meter displays signal amplitude at the various frequency bands of interest that are obtained with a Krohn-Hite bandpass filter interposed between the sensor and the meter. Both the Model 1933 Meter and the filter device are battery powered and portable to field sites as well as usable in the laboratory. All GR 1933 readouts have been manually recorded. A full description of the Fourier analysis processor has been given in Ref. 1.

Accelerometers are mounted onto the solid walls of the channel (usually concrete) by being screwed onto cheap, dedicated, stainless steel mounting studs that have been cemented with commercially available epoxy based adhesives to the concrete surfaces. The obvious advantage of this approach is that many inconspicuous studs may be left at any field test site without concern for potential theft or damage. The prototype system and accelerometer is brought to the test site and activated by test personnel. (A more compact operational system would be mounted on a utility pole).

Our experience with these mounting stud installations in the field includes the October 1977 to August 1978 exposure period. The first stud attachments deteriorated rapidly because the weathered top layer of the concrete surface first had not been removed before cementing; the epoxy adhesive layer was stronger than the underlying cement layer. Our later experience from about mid-November 1977 indicated excellent retention of the mounting stud except where ground level attachment made it subject to accidental mechanical impact by, for example, grounds maintenance machinery. Although the stud face is only about 1/2 inch (1.25 cm) in diameter, it adheres as strongly to a well prepared concrete surface as when it is cemented to a 2 inch (5 cm) square metal plate prior to mounting on the environmental surface.

Accelerometers, of three different output signal sensitivities, provided superior vibration detection (amplitude and frequency range) on the concrete surfaces, nearby to the channel discontinuity, than, for example, neighboring microphones supported to receive primarily airborne sound. In the latter measurement equipment situation, the higher frequency range (e.g., above ~8 kHz) was undetectable.

The most useful accelerometer was a B&K 4332 model because its high sensitivity of 62 mv/g provides strong sensor signals, and its flat frequency response to 50 kHz encompasses the needed working range.

PHYSICAL MEASUREMENTS

The physical measurement of the storm sewer flow in the field used measurements of water velocity at a grid of many points, and the integration of these data, each as representative of a small stream tube, over the entire channel cross-sectional area. The velocity was measured with a Marsh-McBirney Model 201 portable battery-powered, water current meter. This system uses an electromagnetic sensing head. When immersed in water, a voltage field is established around the probe. Electrodes imbedded in the probe body sense the voltage field whose amplitude is proportional to the water velocity around the probe. The electrical signals are transmitted through a cable to a portable processing and meter display unit. The

velocity readouts in the 10 ft/sec (3.05 m/sec) full scale range are real time measurements and certified accurate to ±2%. The meter time constant is only 6 seconds so practical flow rate changes are measurable. A marked mounting rod and support structure allowed the sensing head to traverse, in the vertical and horizontal directions, within 1.5 feet (0.5 m) (upstream) of the exit face of the 60 inch diameter (1.5 m) sewer pipe at the Cutter Mill and Baldwin Creek channels during wet weather flows. The requirement of maintaining at least one inch (2.5 cm) of water around the 1.5 inch (3.8 cm) maximum diameter of the velocity sensor limited its usefulness in dry weather flows. For these cases where the maximum water height in the sewer pipe is only 3 to 5 inches (7.5 to 12.5 cm), a V-notch weir was used (See Fig. 8). Measurement of the maximum height of water crest, H, for the Vee, and use of the equation

$$Q = 2.50\ H^{2.50} \tag{14}$$

allows the volumetric flow rate to be computed. The dry weather flow at Baldwin Creek is so slight, however, that even the V-notch weir was not effective; the flow was estimated as essentially zero, although a slow visible trickle existed.

Figure 8. V-notch weir at Cutter Mill Drain outfall for measuring low flow rates.

From measurements of the maximum water height in the free-flowing 60 inch (1.5 m) diameter Cutter Mill sewer pipe, concurrent with the velocity and measurements, a correlation has been made of flow rate to the water height. The approximate relation, shown by Fig. 9, has been found useful in making quick check assessments of mass flow during an acoustic measurement session.

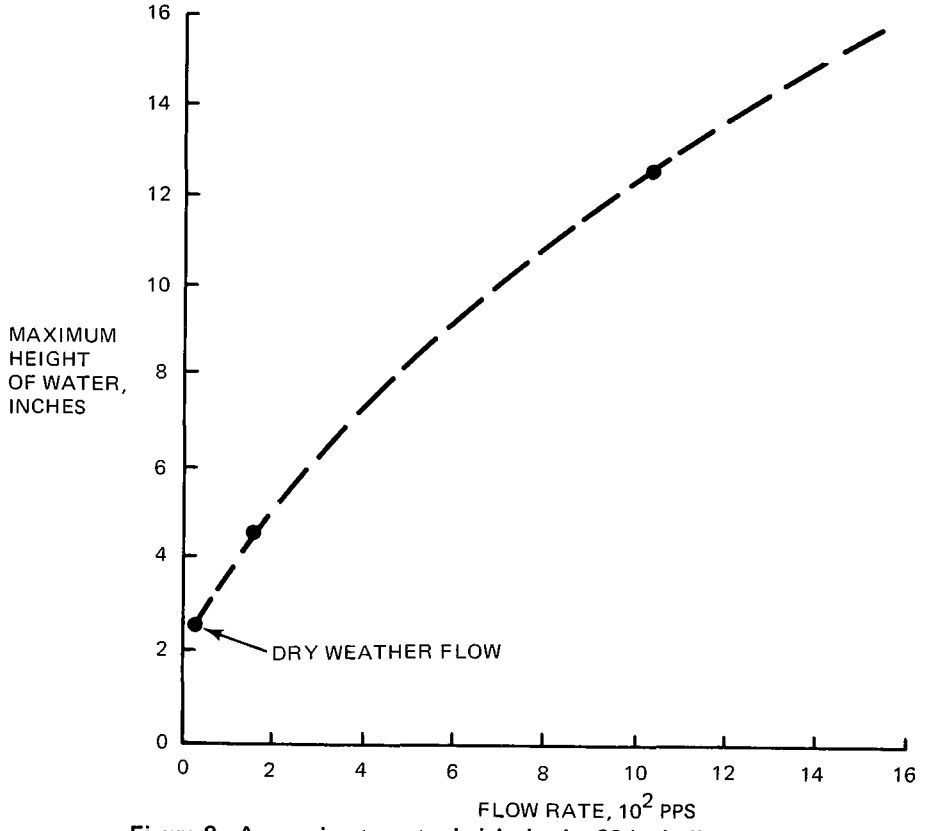

Figure 9. Approximate water height in the 60-inch diameter Cutter Mill Drain sewer pipe corresponding to measured flow rate.

SECTION 6

TEST RESULTS

The format of presentation in this section is to report on the acoustic and flow data by field test site. For each particular site, first the scale model laboratory results are given, and then the field measurements documented. The implications of these combined results then are discussed in a preliminary manner. These results are put into an overall perspective in the following Section 7.

CUTTER MILL DRAIN SITES (LAKE SUCCESS AREA)

Outfall Site

As shown by the diagram and photograph (Fig. 10), three sensor mounting studs (positions 1, 2, 2A) were attached to the head wall and two to the wing wall (positions 3, 3A). Sensor positions 2A and 3A were intended to be closer to the water surface then positions 2 or 3 and therefore to improve the signal strength. However, sample data indicated in actuality no appreciable difference in relative signal intensity. Also, data at position 2 were of a similar nature to that at position 3, therefore, no separate presentation are included here for positions 2, 2A, or 3A. Electrical cables connected the screwed-on accelerometer to the preamplifier, amplifier, and Nagra FM tape recorder. All the electronic components of the prototype system rested on the concrete ledge atop the headwall.

Comparable sensor mounting locations to field positions, 1, 2, and 3 were provided on the 1/20th scale laboratory model. Model position 1, however, was on the model headwall, just above the supply pipe exit face, instead of within and on the roof of the pipe as in the field installation. In addition, the model was provided with sensor position 5, which is a near-mirror image location to position 3, to check flow symmetry; no field sensor location comparable to model position 5 was provided.

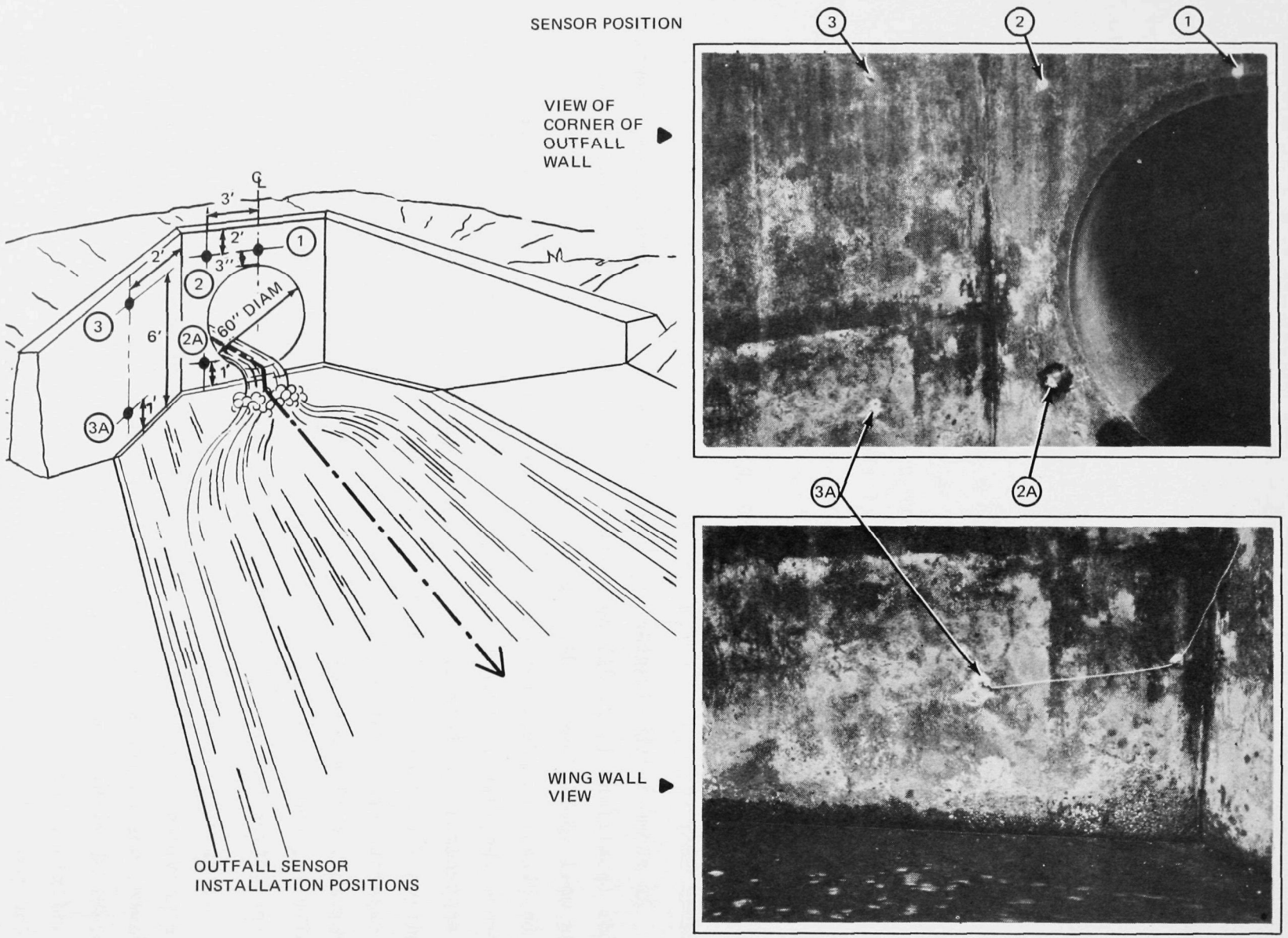

Figure 10. Sensor installation positions at the Cutter Mill Drain outfall.

In the laboratory test series, the height of the step discontinutiy between the supply pipe and the downstream channel model was changed from zero to 1 inch (2.54 cm) by 1/2 inch steps. This investigation was designed to demonstrate the premise of acoustic emission signal amplitude being dependent on a frequency that characterizes the discontinuity. However, data for all three discontinuity heights were not taken at all sensor positions. The changing of the headwall discontinuity was independent of the geometry of the check dam modeled site located about 3 feet (1 m) downstream. It should also be observed that the altering of the vertical step had a very minor influence on the contours of the horizontal (or lateral) discontinuity; the latter channel change also stimulates acoustic emission from the flow but at different characteristic frequencies than the vertical step.

Sensor Position 1

The data obtained at model position 1 (above the supply pipe exit plane centerline) is shown by Fig. 11 in terms of increase in sound decibels (dB) above ambient background noise, for increased weight rate of water flow. (The decibels are computed from the equation $dB = 10 \log (SP/SP_{REF})$, where SP is the sound power of the flow acoustic signal and SP_{REF} is a referenced sound power signal.) The five frequency bands compared by Fig. 11 were taken from the full spectral range processed by the Fourier Analyzer. In general, especially at the lower flow range (0-3 pps) the signal change in dB appears to increase with flow at a higher rate for the 1/2 inch (1.27 cm) step than for the zero step arrangement. At the higher flow rates the difference in sound signal for the two step sizes tends to diminish. The theoretical characteristic frequency in water for the 1/2 inch step is about 59,000 Hz, and it is indeterminately greater for the zero step condition. Therefore, the observed peaks in the overall spectral distribution shown by Fig. 9 must represent higher harmonics, or characteristic frequencies arising from other dimensions of the model such as the lateral change in flow channel area. In the latter case the increased signal from the larger vertical drop condition represents the greater pressure fluctuations (or local pressure drop) associated with increased impact effect from higher

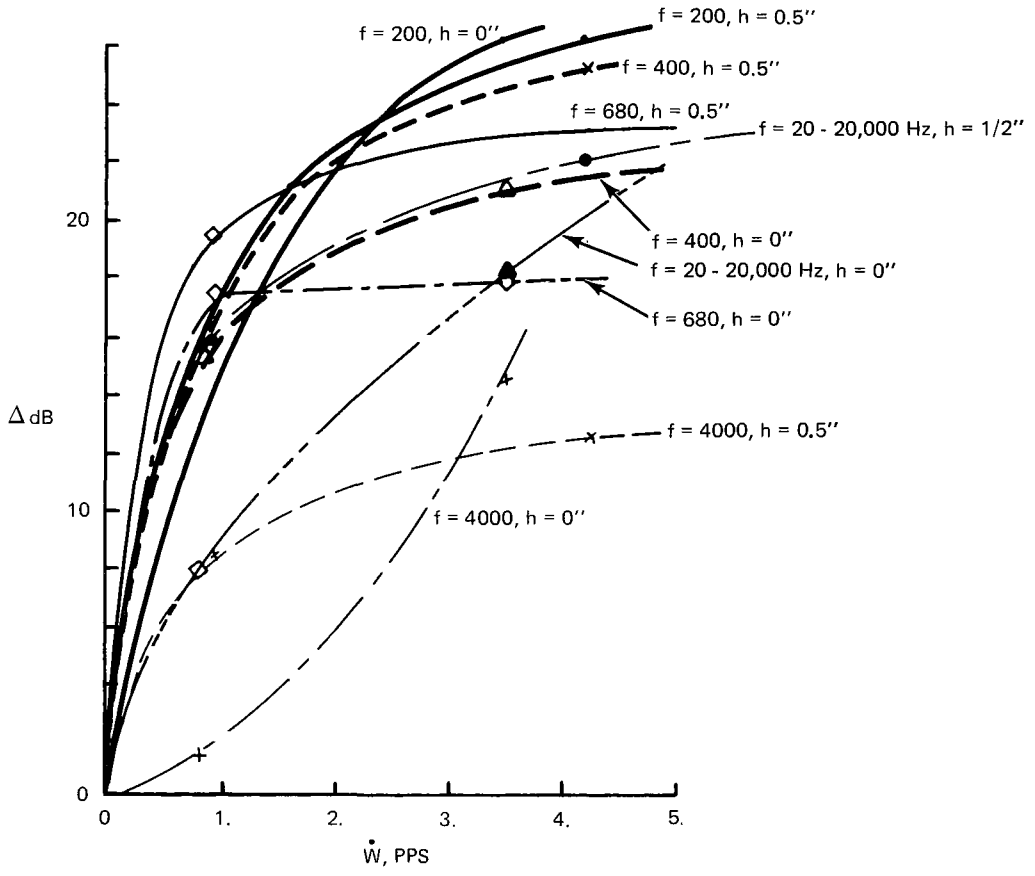

Figure 11. Acoustic signal vs flow rate at position 1 for the 1/20th scale model of the Cutter Mill Drain outfall.

water falls. A portion of these pressure losses are converted into acoustic energy that radiates as a dipole. The greater signal at the lower frequencies probably arises from the lower transmission loss of sound through the model walls at the lower frequencies. For example, the indicated actual exponent relating sound power to mass flow rate, from these model tests with a 1/2 inch step is 1.24 at a frequency of 400 Hz and 0.62 at a frequency of 4000 Hz. Both determinations were made for the flow rate range of about 0.8 to 4.2 pps, corresponding ideally to full scale flows of 320 to 1680 pps (2300 to 12,000 gpm), prespectively. The 50% lower exponent at the higher frequency is attributable to the wall transmission loss as well as different acoustic conversion mechanism efficiency.

The corresponding field site data at position 1 is given by Fig. 12 for five frequency bands. The sound power, in dB, increases with increased flow rate above dry weather flow (22 pps).

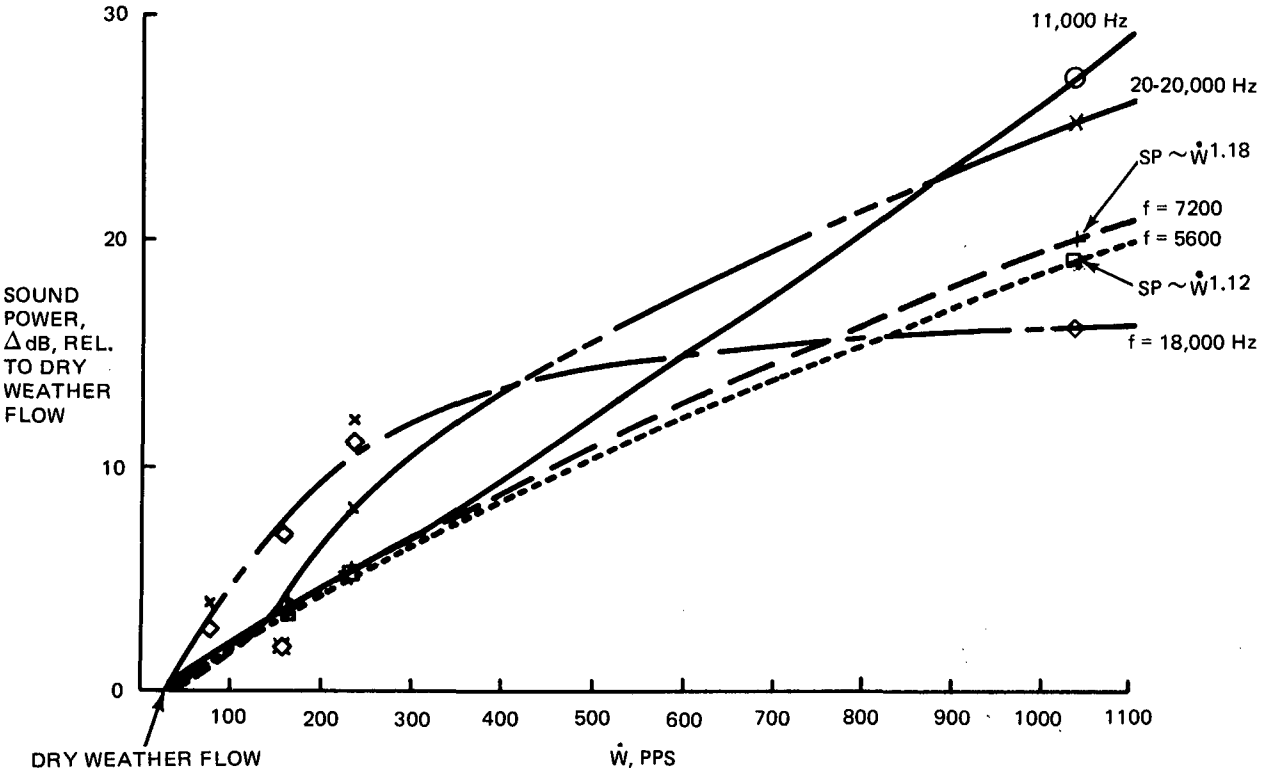

Figure 12. Acoustic signal vs flow rate at field site position 1-Cutter Mill Drain Location.

In the frequency band between 5600 and 7200 Hz, the sound power varies with flow rate approximately as the 1.15±0.03 power over the experienced flow rate range. As becomes evident by studying Fig. 13, which displays the approximate spectral distribution of acoustic emission differential between the maximum wet weather flow (1040 pps ≃ 7500 gpm) and dry weather flow (22 pps ≃ 160 gpm), the peak or characteristic frequency of the field site is at about 11,000 Hz. The sound power varies overall at the 1.6 power of flow rate at this characterizing frequency. The emitted sound is greatly attenuated at higher frequencies (up to 18,000 Hz) because the higher flow rates impact the channel bed further away from position 1 than at lower flows; the longer transmission path in the concrete reduces the signal strength. Over a lower flow rate range, between 230 and 22 pps (1650 and 160 gpm), the flow impacts closer to the exit face and the channel wall

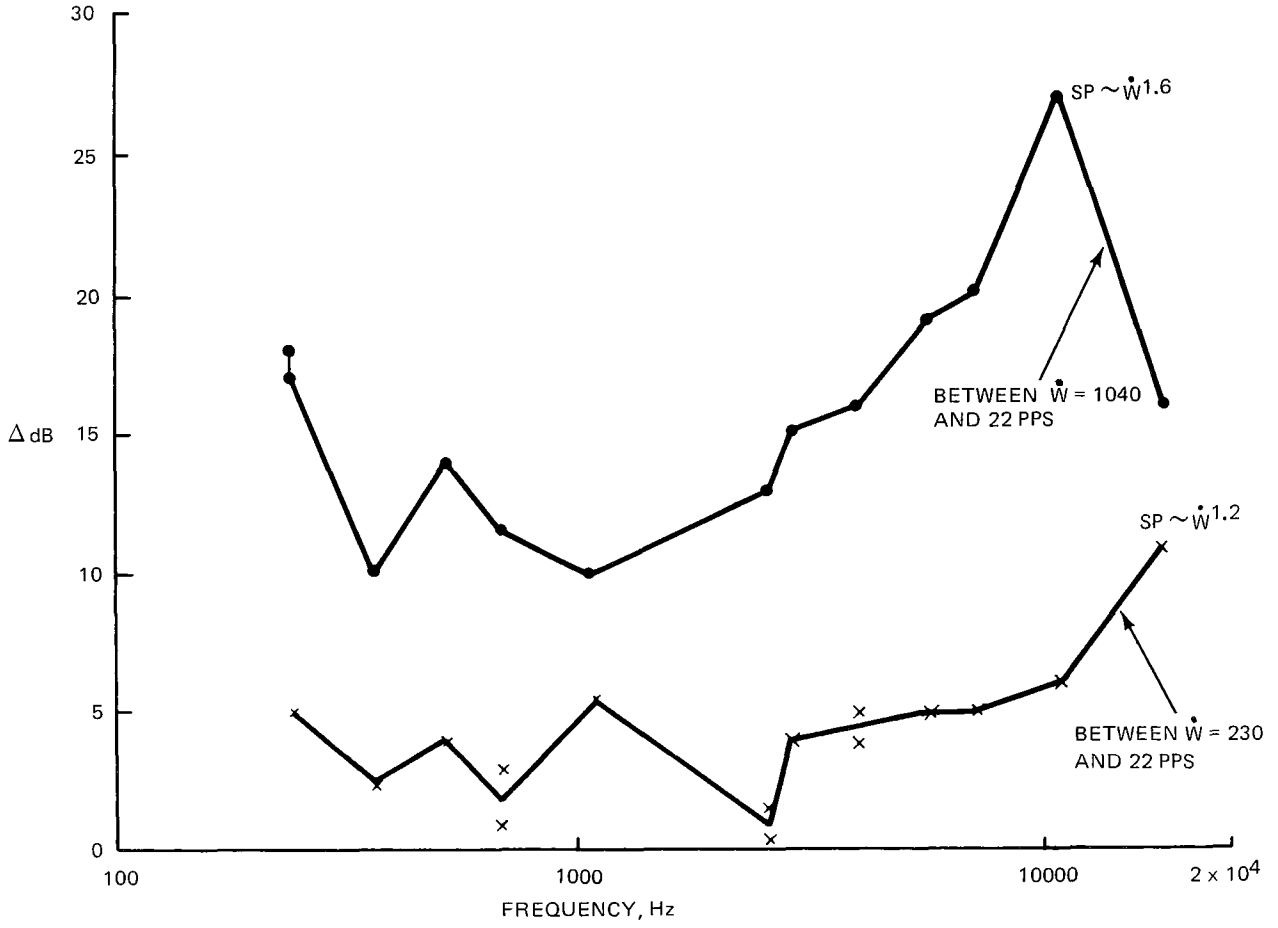

Figure 13. Spectral distribution of acoustic signal for two flow rate differentials at field site position 1 Cutter Mill Drain outfall.

attenuation is relatively less severe at high frequencies. The exponent of flow rate in this lower flow rate range is 1.2 at a characteristic frequency of 18,000 Hz.

Sensor Position 3

Model test results monitored at wing wall position 3 are presented by Fig. 14 for three frequencies bands and three step discontinuity heights. As we evidenced at position 1, the higher step (i.e., 1 inch (2.54 cm)) produces greater sound intensity above background noise for all flow rates compared to the lower step height conditions. The frequency band-center yielding the greatest increase in flow acoustic emission intensity, above the laboratory background noise, is at about 2900 Hz for position 3. The increase in intensity with step height for the high range laboratory

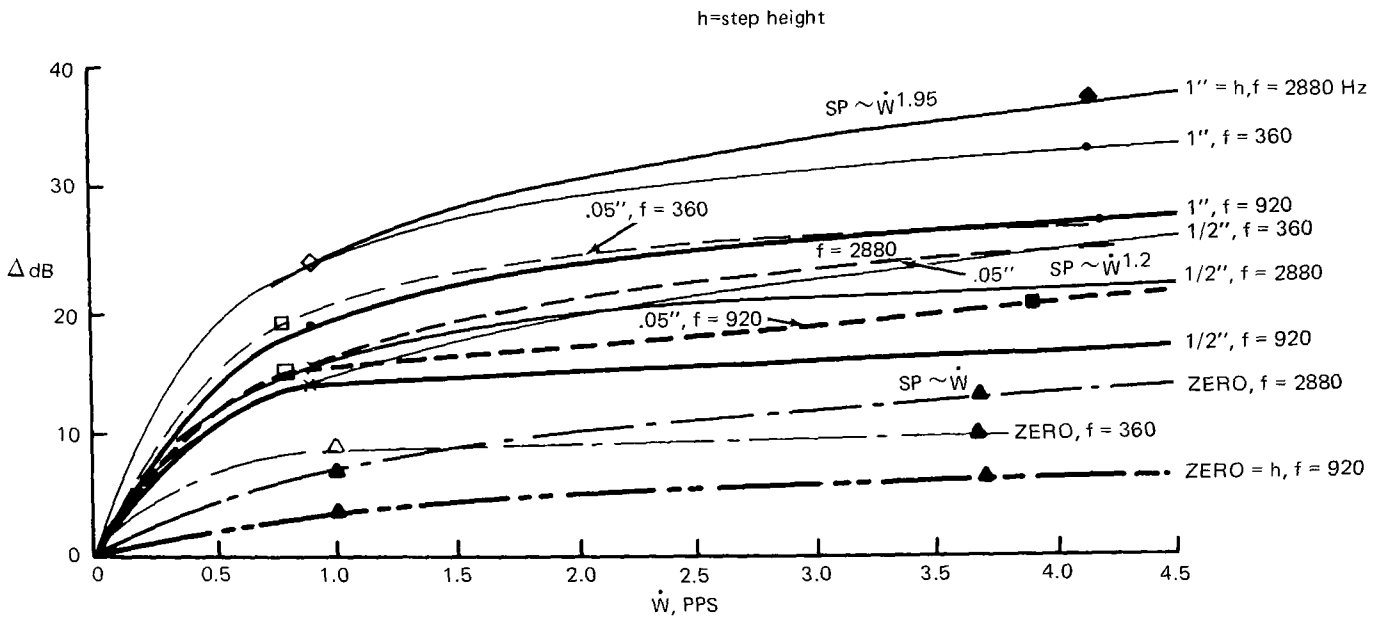

Figure 14. Acoustic signal vs flow rate at position 3 for the 1/20 scale model of the Cutter Mill Drain outfall with different step sizes.

flows (i.e., ~ 3-4 pps), is approximately linear at 10 ± 2 dB per 0.5 inch (1.77 cm) of step. Model flow sound power varies with flow rate to the 1.2 power at the 1/20th scaling, over the range of flows tested, but at a 1.95 power at 1/10th scaling of the discontinuity step, for a frequency of 2900 Hz. For no step discontinuity, the flow sound power varies as flow rate. These results and the observation that 2900 Hz corresponds to a characteristic wavelength in water of about 20 inches (51 cm), or even numbered fractions thereof for harmonics, makes it evident that this frequency probably is not linked directly to step height. More likely 2900 Hz results from the increase in flow channel (horizontal plane) width at the discontinuity (i.e., approximately 5 inches (12.7 cm). The larger signal intensity at larger step heights then represents a modulation (or augmentation) of the basic acoustic emission signal because of the greater level of pressure fluctuations (greater pressure loss) produced by the higher water falls. Further support of this conclusion is the fact that (see Fig. 15) that the signal intensities at about 6000 Hz (i.e., second

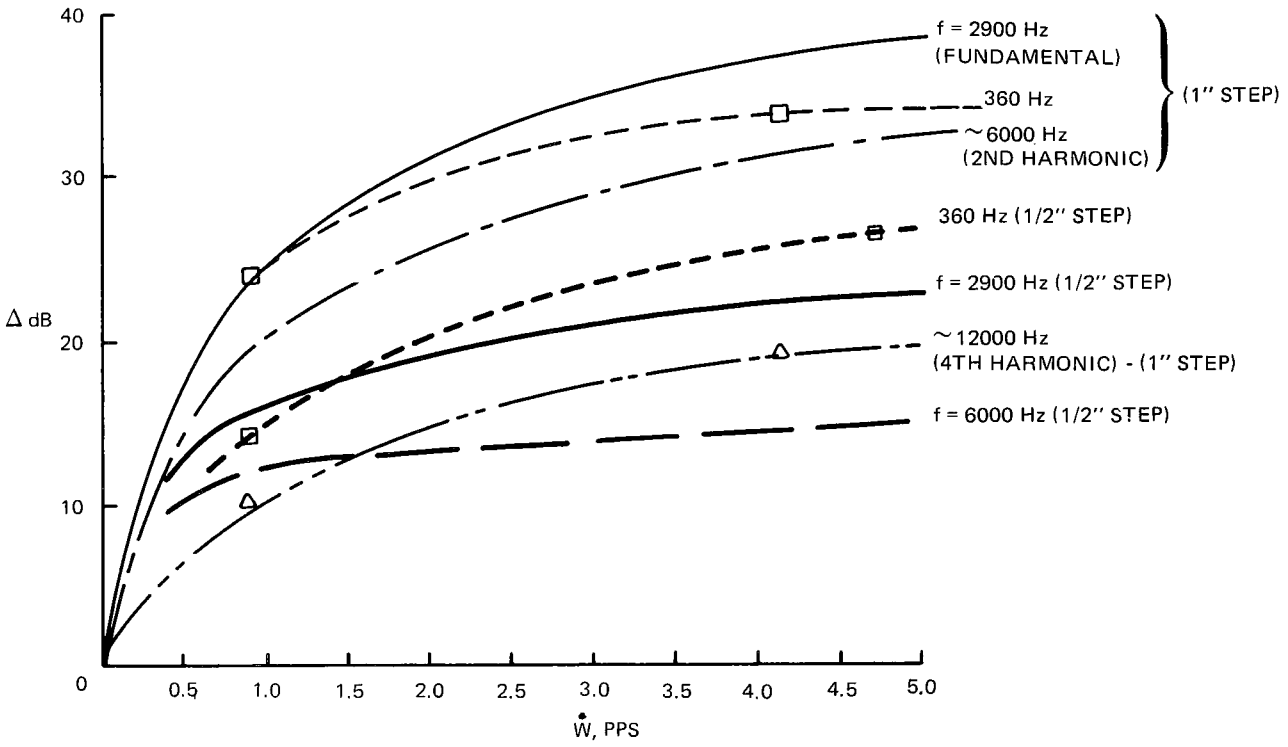

Figure 15. Additional data of acoustic signal vs flow rate at laboratory model position 3-for Cutter Mill Drain outfall geometry

harmonic) and 12,000 Hz (4th harmonic) are virtually at about fixed decrements below 2900 Hz; these decrements can be attributed to the channel wall transmission loss coefficients which are only frequency dependent and which exhibit greater loss at higher frequency. On the other hand, at a frequency of 360 Hz (1/8th the assumed fundamental) the signal falls off by a variable amount depending on flow rate above about 1 pps. The sensor signal at Model position 3 also was processed by the GR 1933 signal analyzer. A comparison of the GR 1933 meter (used with a Krohn-Hite Model 3700 filter) readings to the Fourier Analyzer results (see Fig. 16) indicates fairly good agreement for all frequencies below about 4000 Hz. The data at about 2600 Hz has the best agreement. The spread in results at, for example, 6000 Hz and above probably can be attributed to the filter

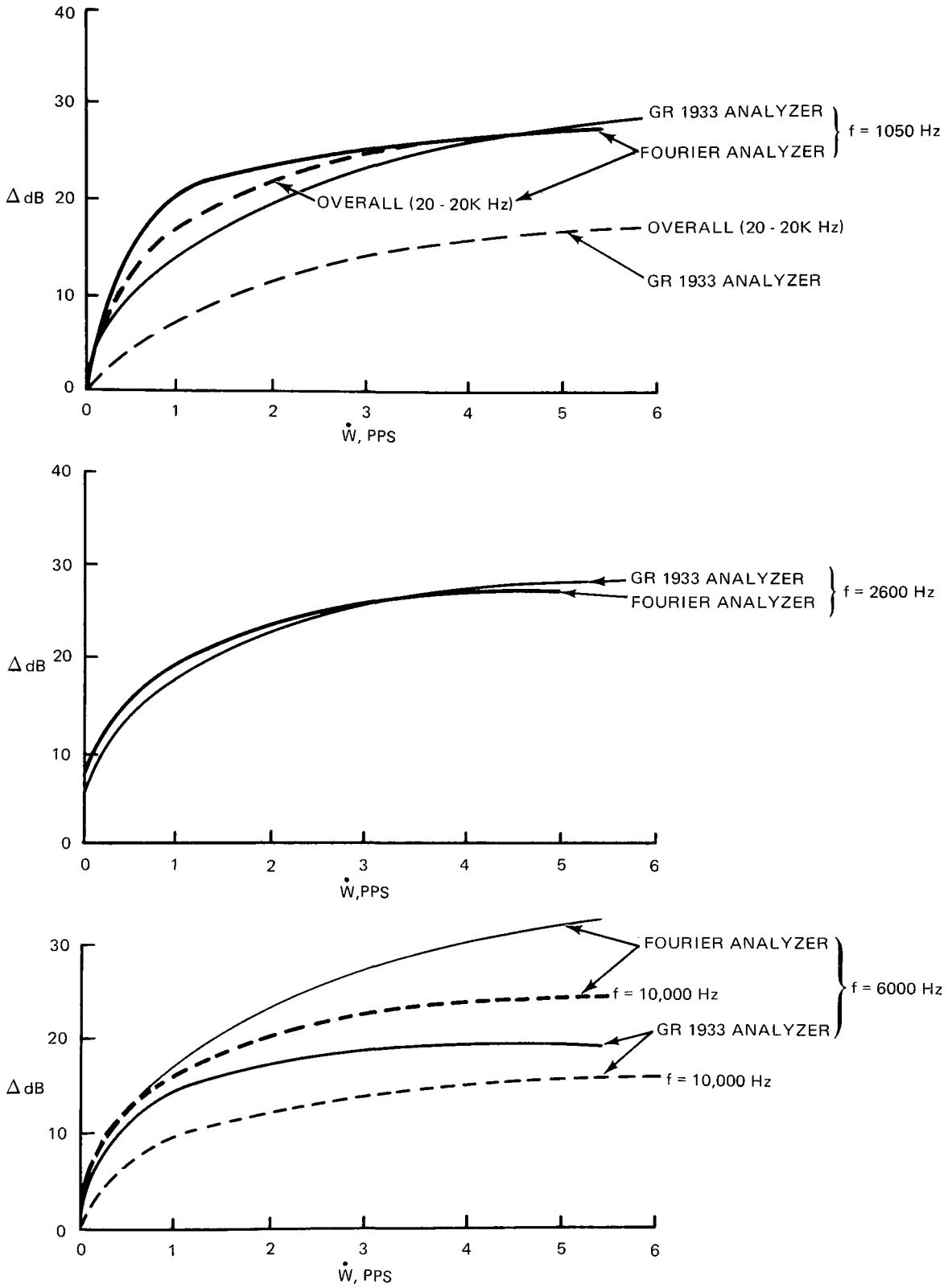

Figure 16. Comparison of Fourier Analyzer - processed acoustic signals with GR-1933 meter measurements at laboratory model position 3-for Cutter Mill Drain outfall geometry

unit's cut-off pattern. One of the operating characteristics of the Krohn-Hite filter is that if the adjustable high frequency and low frequency filtering limits are set too close (e.g., on a central frequency) the net output signal is 6 dB lower than the actual input signal. The comparative signal values for the model's overall frequency band between 20 and 20,000 Hz) are approximately 10 dB apart over most of the flow rate range, with the GR 1933 measurements lower than the Fourier Analyzer results.

The exponent for 1/20th scale model flow rate in the sound power relationship is 1.89 at a frequency band centered about 1050 Hz, 1.35 at 2600 Hz, and 2.43 at 6000 Hz. In the field, sensor position 3 on the wing wall is about 6.7 feet (2.0 m) from the bottom lip of the sewer pipe centerline instead of a few inches as in the model. Then, the distance correction needed to be added for the field data is about 9 dB for very low flows and about 8 dB for the high flow rates in order to correlate properly with laboratory model test data.

The field test data given by Fig. 17 at two frequencies show an increase in sensed signal which increases to the 0.95 power of flow rate (for 18,000 Hz). If an 8 dB correction for distance is made, the source of the acoustic emission signal would appear to vary with flow rate to the 1.4 power at a frequency of 18,000 Hz. Because the characteristic frequency in water of the 10 inch (25.4 cm) step at the outfall is about 6000 Hz, the data given at 18,000 Hz would be third harmonic results. However, an examination of the approximate spectral distribution of intensity of field signal, shown by Fig. 18, indicates that the peak intensity at about 6000 Hz is about 3 dB lower than the peak at 18,000 Hz. Normally, the intensity of harmonics are less than at the fundamental mode. While it is true that sensor installation resonance could be the cause of the higher signal, this point has not been demonstrated a posteriori. On the other hand, the second harmonic which would occur at about 12,000 Hz is not evident from the field data. However, this omission, in itself, is not an invalidating reason because, often, only odd harmonics are excited in large structural systems.

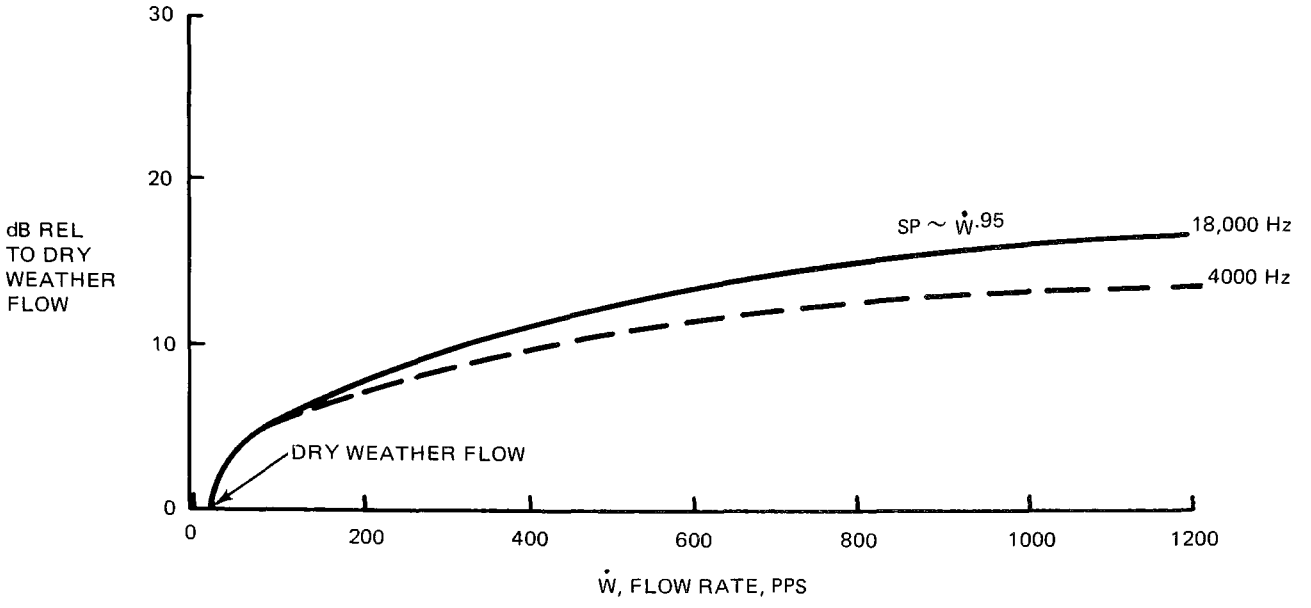

Figure 17. Acoustic signal vs flow rate at field site position 3-Cutter Mill Drain outfall.

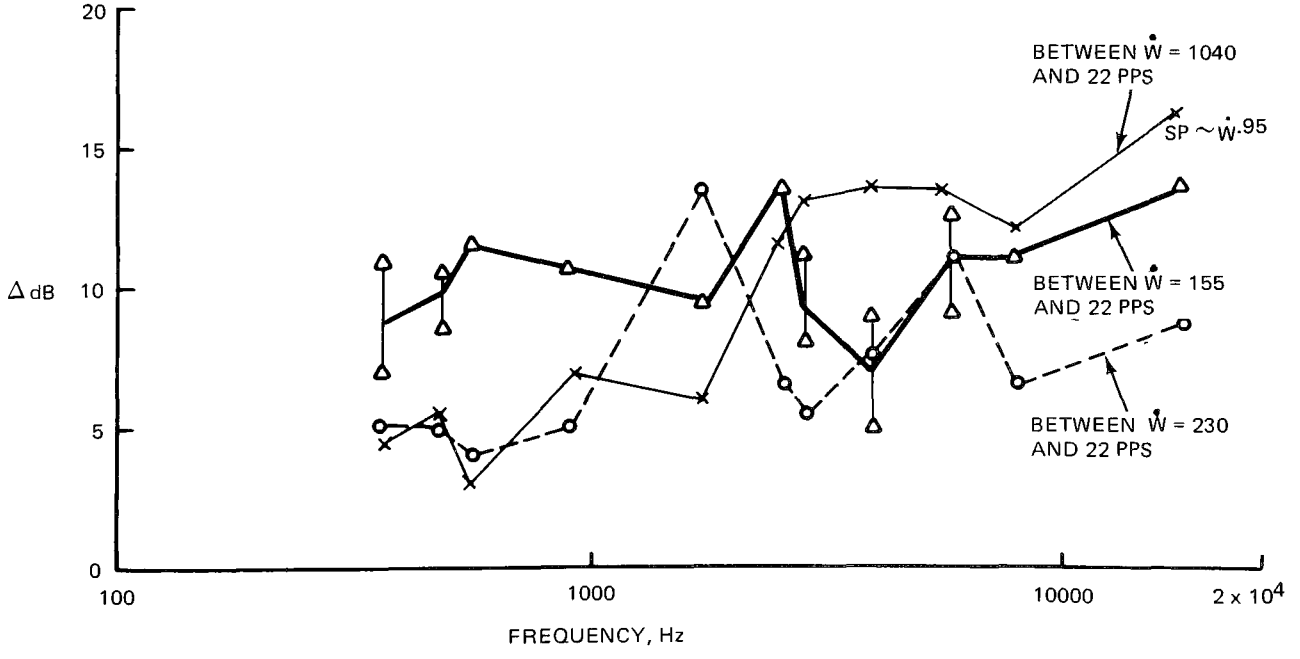

Figure 18. Spectral distribution of acoustic signal for three flow rate differentials at field site 3-Cutter Mill Drain outfall.

It should be noted that the laboratory model's dimensions would create a 1-inch (2.5 cm) step-induced characteristic frequency of almost 60,000 Hz which could not be recorded because it exceeds by a considerable amount, the working range of the tape recorder and sensor. For this reason, the frequency-simulation of the field installation could not be accomplished by geometrically similar small scale laboratory models. Exaggerating the vertical scale at the discontinuity, to create a step of 3.5 inches (8.9 cm) or more, would bring the frequencies into the working range, but might have created other problems of geometric distortion. For this reason, in analyzing the small scale model data, the other and larger dimensional discontinuity features that also could induce concurrent acoustic emission mechanisms, but at measurable frequencies, were used.

Any other explanation of the field data trend at 18,000 Hz except for sensor installation resonance, fails to explain the variation of signal intensity from the dry weather (22 pps) to 1040 pps flow range. Clues to another source mechanism is suggested by the data for the 230 to 22 pps flow range in Fig. 18. Intensity peaks at 1800, 6000, and 18,000 Hz suggest the effective flow discontinuity to be the horizontal spread of the pipe flow into the open channel (i.e., from a 2.5 foot (1.5 m) radius to a 5 foot (3.0 m) channel half-width). Then the decrease of relative intensity with third harmonic (at 6000 Hz) and with ninth harmonic (at 18,000 Hz) are consistent with a generally expected trend. However, this alternative explanation breaks down for the higher flow range data.

Because of the inability to model signal frequency, the model and field data cannot be completely and neatly correlated. However, the fact that source sound power for both size scales of channels are proportional to flow rate to a power of between approximately 1.0 and 2.0 seems to confirm the similarity of source mechanism. The location of the sound emission generally in the audible frequency range, and below ultrasonic, also confirms the pseudosound, dipole type, origins of the measurements.

Sensor Position 5

This mounting stud location is close to the mirror image of position 3 on the opposite side of the laboratory scale wing wall. However, it is

slightly more downstream than position 3. No comparable data were taken at the field site.

The variation of sound intensity with flow rate is shown for a frequency of 2760 Hz by Fig. 19. In similar fashion to data at position 3, the intensity at position 5 increases about 10 ± 2 dB per 1/2 inch (1.27 cm) of model discontinuity step. The exponent of variability with flow rate is 1.54 compared to a 1.95 exponent for position 3 and similar frequency (2900 Hz) with a 1 inch (2.54 cm) step. Comparison of other step sizes for the two positions is given by Fig. 20, and show excellent correlation. These data indicate the uniform distribution of the acoustic emission with geometric symmetry of the flow channel. Other data at frequencies of 360 and 7200 Hz, not shown, also yield similar results.

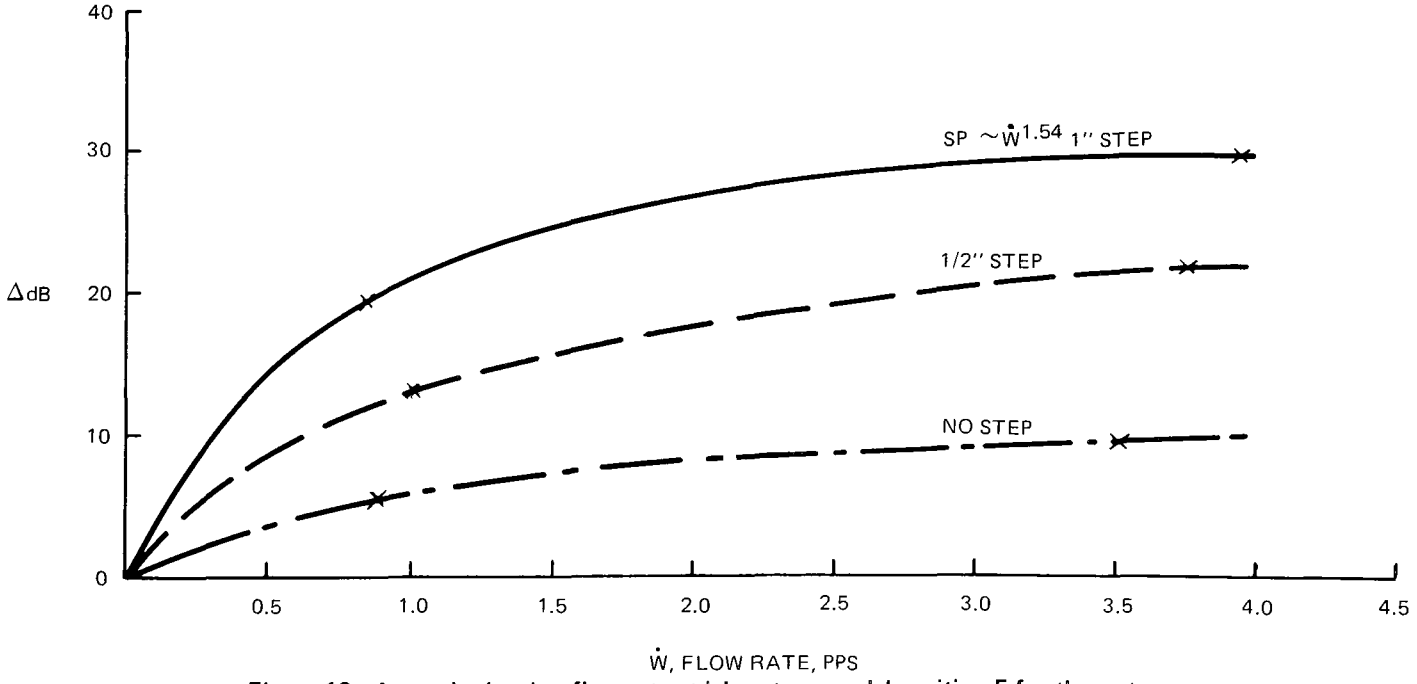

Figure 19. Acoustic signal vs flow rate at laboratory model position 5 for three step sizes at a frequency of 2760 ± 100 Hz - for Cutter Mill Drain outfall geometry.

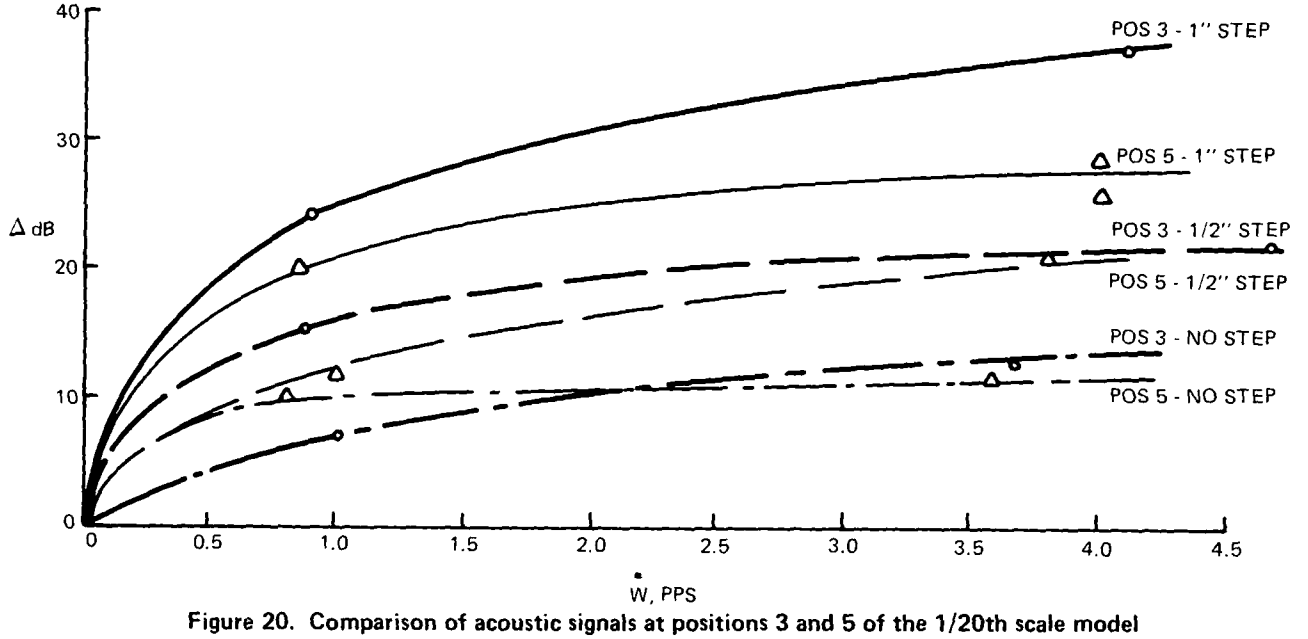

Figure 20. Comparison of acoustic signals at positions 3 and 5 of the 1/20th scale model of the Cutter Mill Drain outfall geometry at a frequency of 2900 ± 100 Hz.

Check Dam Site

This location was the second of three field channel discontinuity sites investigated. As shown by the diagram and photograph (Fig. 21), sensor mounting studs were attached to the downstream vertical wall of the check dam (position 12) and on the right cemented bank (position 20) about 5 feet (1.5 m) downstream of the spillway lip. In addition, sensor mounting studs were cemented to the concrete flanks (positions 6 and 7) of the spillway. However, the only field position for which acoustic data were obtained over the entire range of flow rates was at position 20. For some of the other locations the mounting stud did not remain attached to the check dam during a test because of what proved to be inadequate preparation of the concrete substrate.

Sensor position 20

Data taken at model position 20 are given in Figs. 22 and 23 for five different frequencies. Although the step in the upstream channel discontinuity should have had no influence on the acoustic emission at the check dam, evidently there was a carryover effect as the plotted data clearly indicates. Because no data were taken in the laboratory with the check dam section replaced by a straight section, we cannot accurately assess how much of the pseudosound radiation is converted into sound carried along by the flow to the vicinity of the check dam, about 3 feet (0.91 m) downstream. However the 9-10 dB sound difference (at the highest of flow rates) for the 1 inch (2.54 cm) step differential indicates a possible 50% conversion efficiency of the original measured outfall source sound production rate of 20 dB per inch. At low flows, (i.e., at up to 1 pps) there appears to be very little effect of the upstream step because, presumably, the absolute level of acoustic emission was weak enough to be completely dissipated.

The strongest acoustic signature at the check dam model is at 1920 Hz frequency and a second harmonic is observed at 3800 Hz. The signal at 960 Hz is about 1/3 less than at 1920 Hz, indicating that it is not likely to be the fundamental frequency of the check dam's acoustic signature.

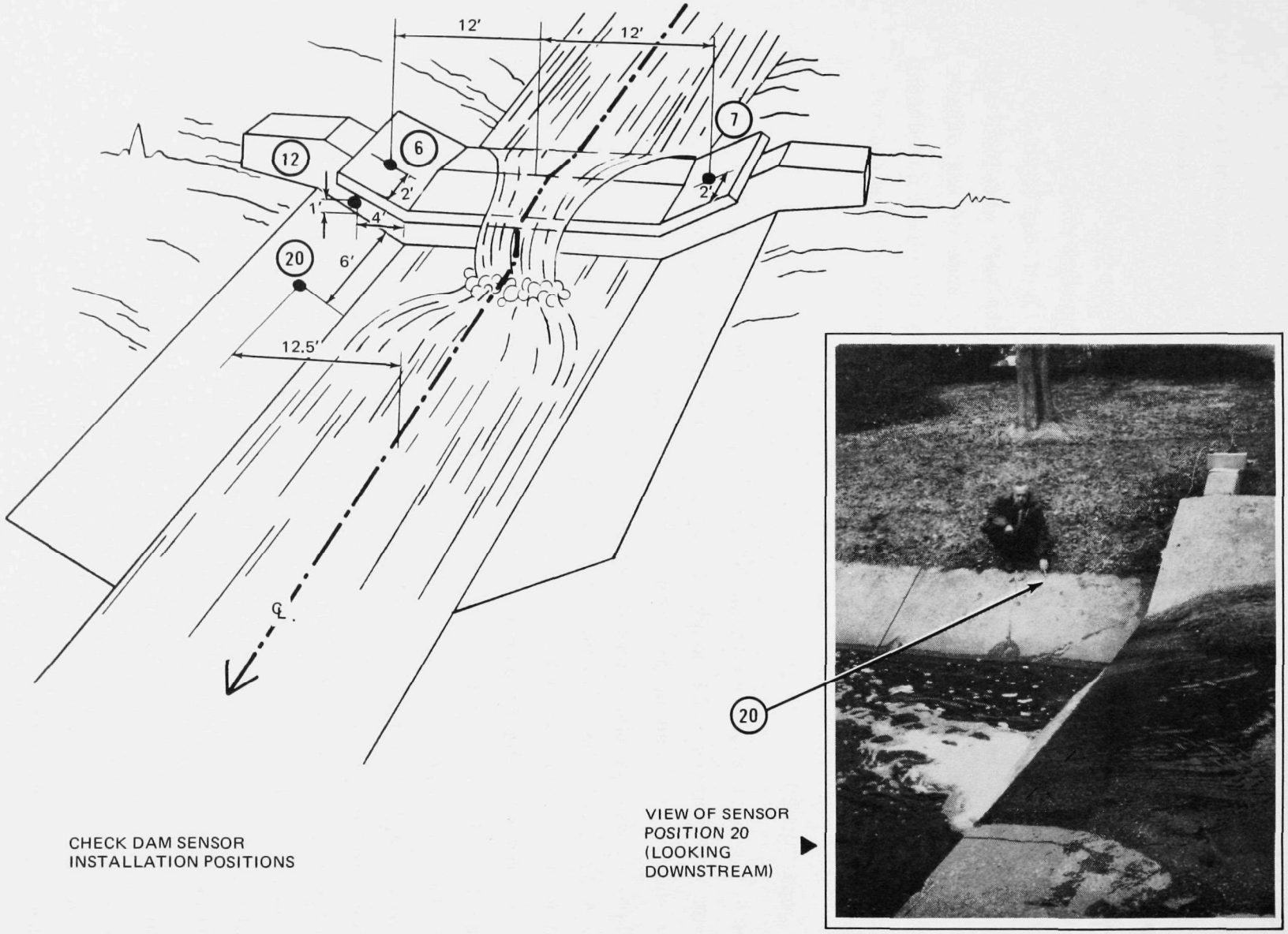

Figure 21. Locations of acoustic sensor mounting stud installations at the Cutter Mill Drain check dam.

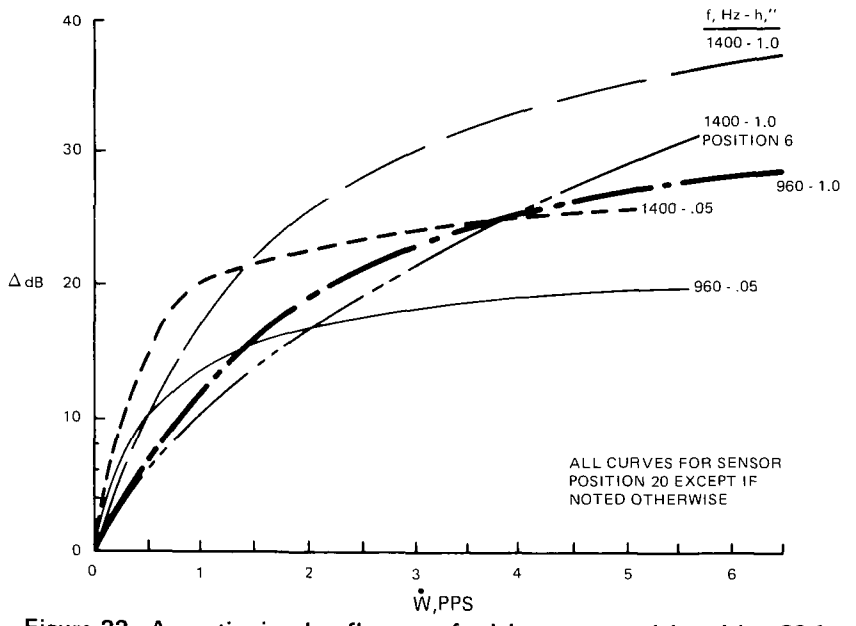

Figure 22. Acoustic signal vs flow rate for laboratory model position 20 for two upstream step sizes - Cutter Mill Drain check dam geometry.

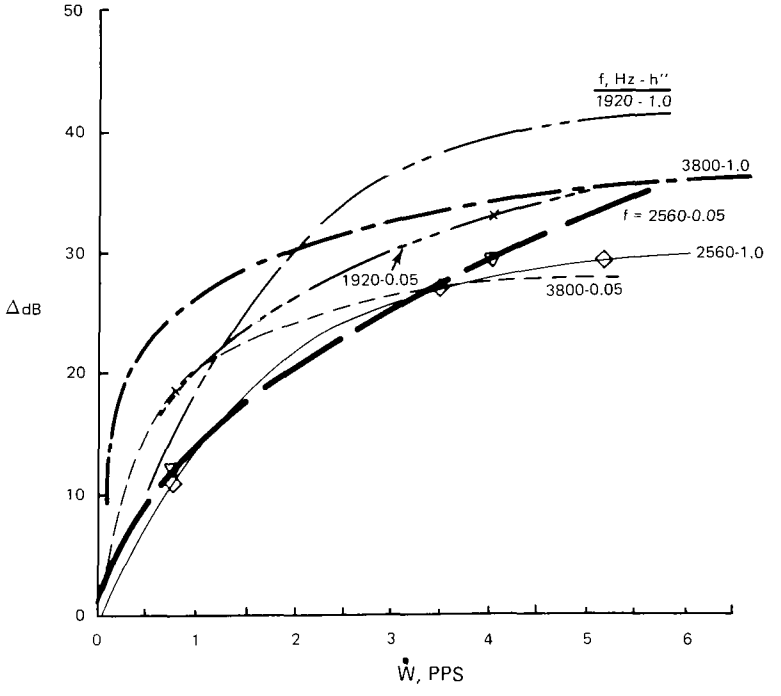

Figure 23. Additional data of acoustic signal vs flow rate at laboratory model position 20 - for Cutter Mill Drain check dam geometry.

The sound power appears to vary to the 2.9 power of flow rate at 1920 Hz; the exponent of flow rate is about 2.5 at 1400 Hz, 2.2 at 960 Hz, and 1.9 at 3800 Hz. These observed exponents are the closest to the theoretical fourth power law for dipole sound radiation, and indicate the closest approximation to an ideal pseudosound production situation created in the laboratory. Once again, the characteristic dimension in water of the model check dam step is associated with a frequency of about 59,000 Hz. Because this value is well above the instrumentation capabilities, other acoustic emission frequencies observed in the test data have been used for correlation with physical flow rates.

The field site sensor position 20 test data are presented by Figs. 24 and 25. The latter is an approximate spectral distribution curve that reveals peak trends of fundamental frequencies and their harmonics. Over the full maximum range of flow rates (1040 to 22 pps), the fundamental frequency appears to be 3800 Hz which corresponds to a characteristic wavelength in water of 15.5 inches (39.4 cm). This dimension is about equal to the actual free waterfall distance from the check dam spillway to the downstream pool, and is confirmatory data on the basic pseudosound mechanism creating the monitored acoustic signal. A third harmonic peak at 11,200 Hz also is evident from Fig. 25 and it exhibits the expected lower intensity, in this case about 7.5 dB less. A fifth harmonic which would be at 19,000 is just beyond the actual range of data presented but the trend of Fig. 25 appears to indicate a reasonable expectation of encountering

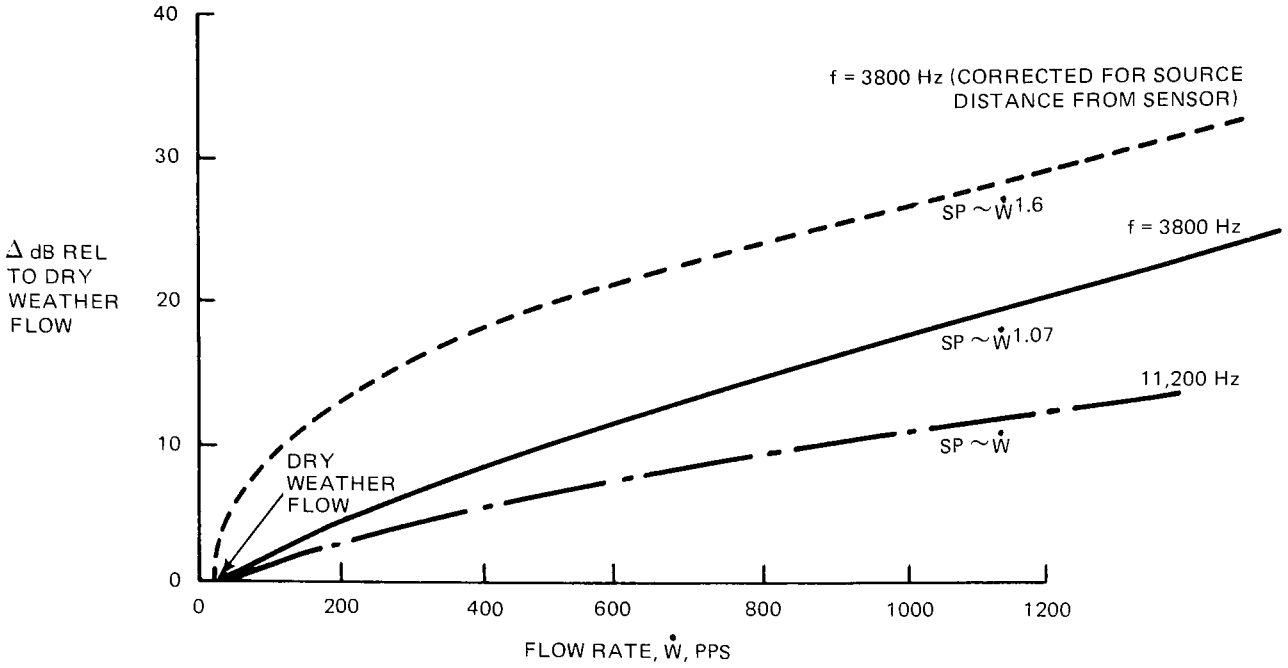

Figure 24. Acoustic signal vs flow rate at field site position 20 - Cutter Mill Drain check dam.

this frequency if the instrumentation and data processing capabilities so permitted. The exponent relating flow rate to sound power at 3800 Hz is 1.07 if no correction is made for physical distance of the sensor from the effective source of the acoustic emission (i.e., the water fall). With a correction of about 9 dB for the 9.5 foot (2.6 m) distance, the flow rate exponent becomes 1.6 for the sound power at the source. Coincidently, this value is in close agreement with the laboratory scale model exponent of 1.9 at 3800 Hz, where distances were too short to require correction.

Sensor Position 6

Data obtained with the laboratory scale model at sensor position 6 is shown by Fig. 26 for several frequencies and two upstream step sizes. Representative comparative data for sensor position 7 also are given. These results are in general agreement with the trends observed at position 20 but are of lower intensity. This smaller signal is understandable for a number of reasons, most notably a) the sensor positions are upstream of

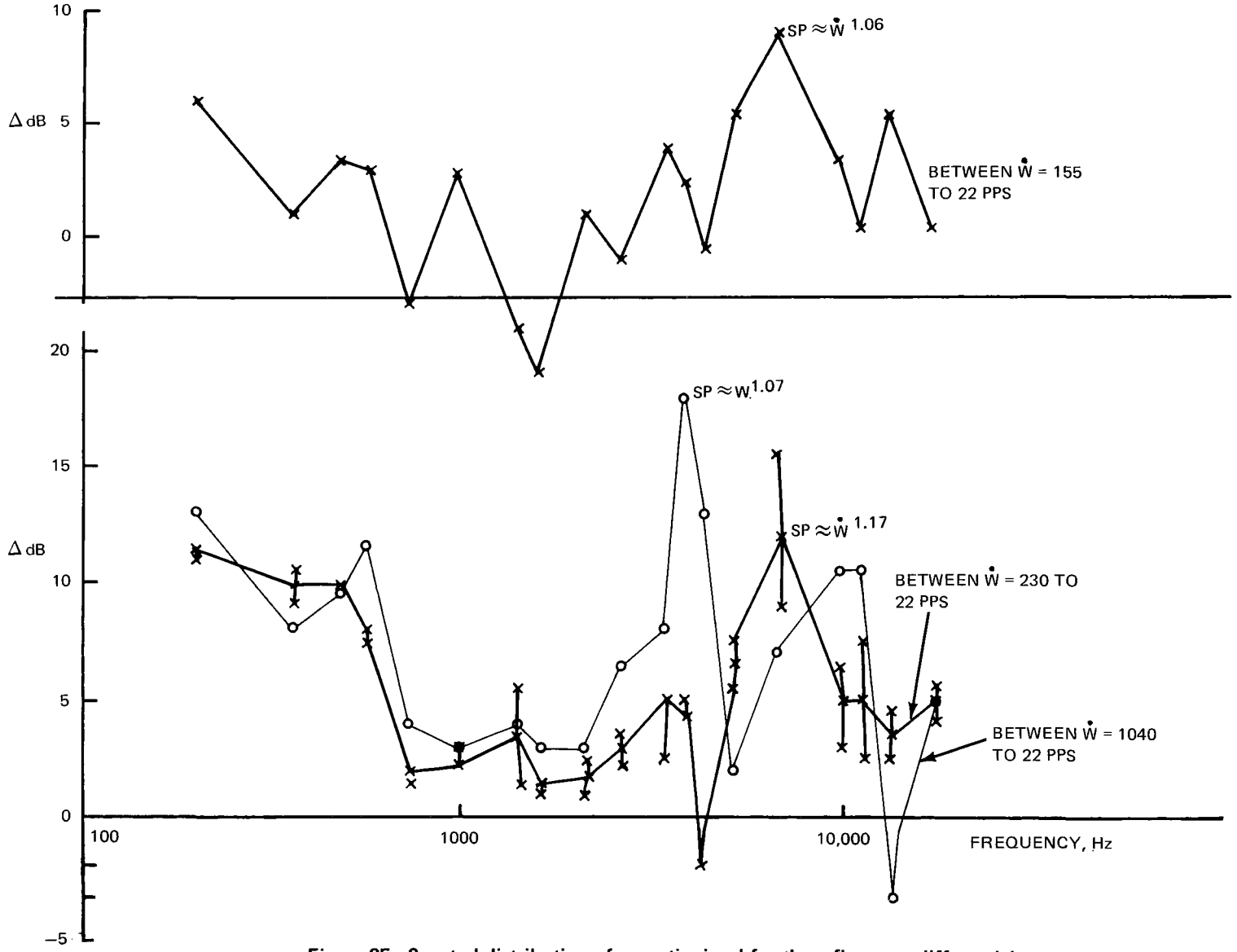

Figure 25. Spectral distribution of acoustic signal for three flow rate differentials at field position 20 - Cutter Mill Drain check dam.

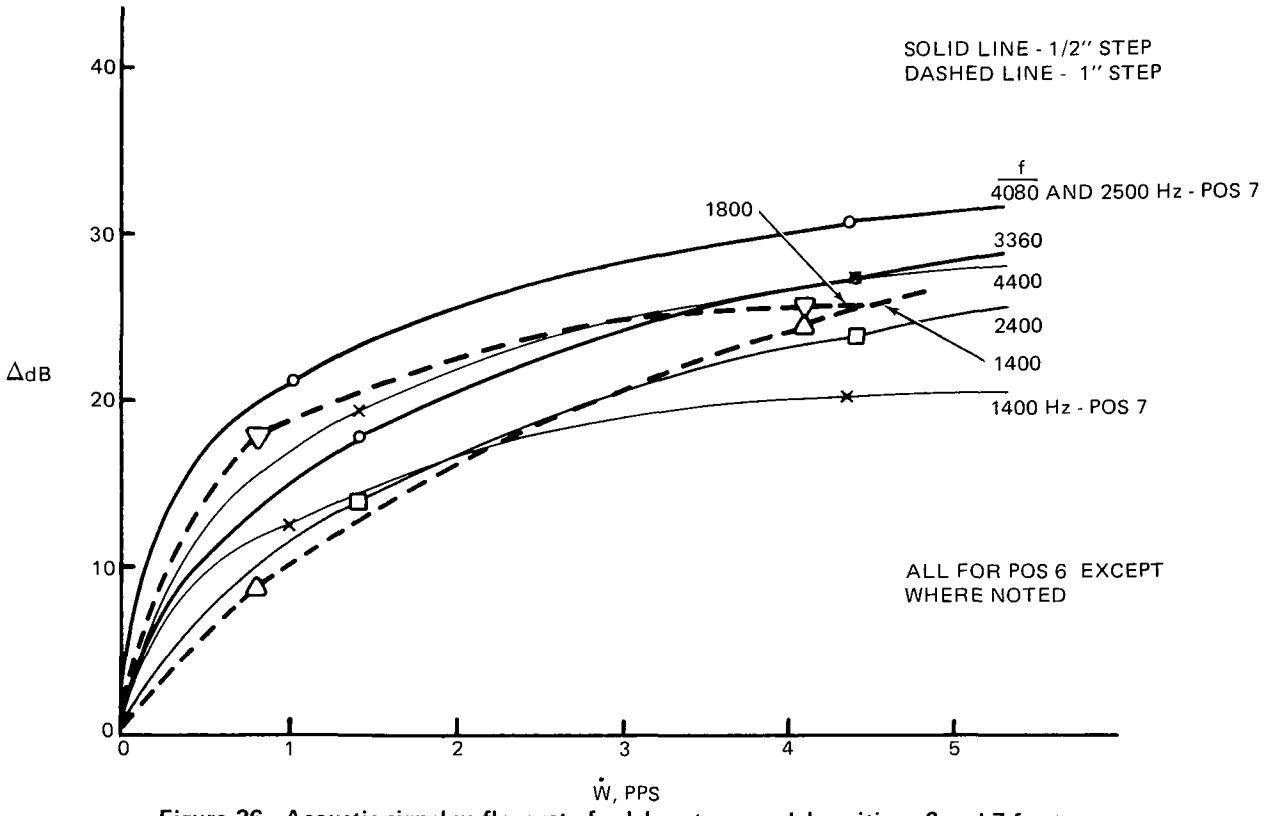

Figure 26. Acoustic signal vs flow rate for laboratory model positions 6 and 7 for two upstream step sizes - Cutter Mill Drain check dam geometry.

the actual discontinuity; b) the positions are further away from the waterfall impact location than at position 20. In addition, at high flow rates position 6 can become wetted by water level surges.

In view of the less favorable circumstances attendant to installation of sensor mounting pads on the exposed flanks of the check dam, only a limited examination was made at positions 6 and 7; greater attention was directed to position 20.

BALDWIN CREEK SITE

100 Degree Turn

The locations of sensor mounting studs at the Baldwin Creek field site are shown by the outline drawing (Fig. 27). Sensor position 4 is located

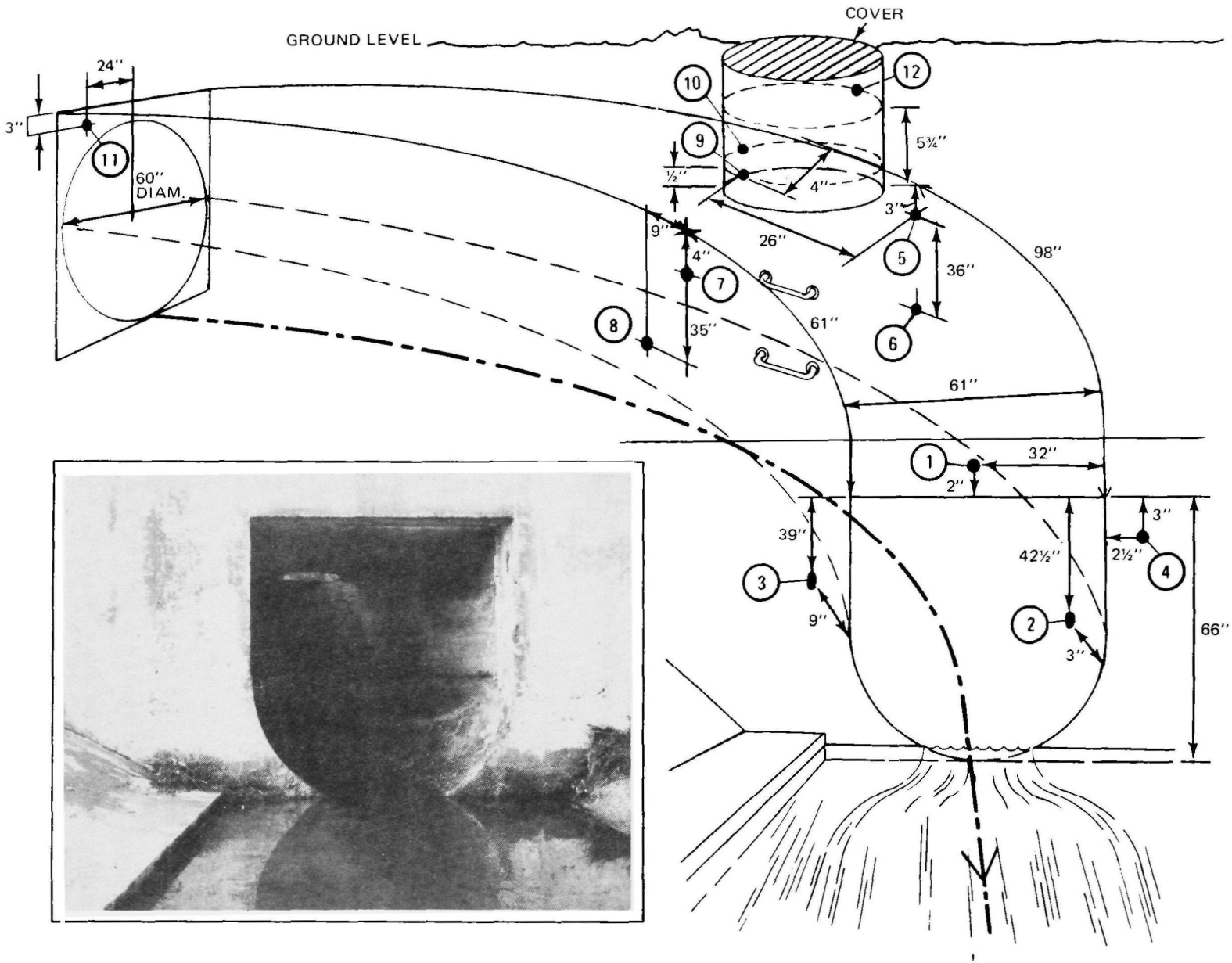

Figure 27. Sensor installation positions at the Baldwin Creek 100 degree turn section field test site.

on the reinforced concrete headwall, at the outfall to the open channel, and about 3 inches (7.6 cm) from the roof and lip of the outfall. Positions 1, 2, and 3 are upstream, within several inches, of the outfall and on the roof centerline, east and west walls (outer and inner radii), respectively, of the reinforced concrete turn section.

Sensor locations 5 through 8 are located roughly midway through the turn with the odd numbered location near to the roof and the even numbered positions at about mid-channel height of the outer and inner radii walls, respectively. Our visual evidence of severe erosion of the lower part of the east (outer radius) wall indicates that for severe stormwater flow conditions the high velocity profile is skewed toward the turn location near position 6.

Sensor positions 9, 10, and 12 are located in the vicinity or on the inner walls of the manhole chimney. Any of these three locations could serve as an indicator of the general suitability of manholes for field sensor installation. Finally, sensor location 11 is on the downstream surface of the headwall joining the 60 inch (1.5 m) diameter concrete sewer pipe to the 100 degree turn section.

In the laboratory the general geometric features of the Baldwin Creek turn section have been duplicated (see Fig. 7). However, because of small size and spatial limitations, faithful duplication of the inner wall installations of sensor mounting studs was compromised; all sensor studs on the model were cemented to the outer surfaces of the turn model at the approximate relative location of the field installation. The relatively thin wall of the laboratory model was expected to make transmission loss small enough to make the external surface pickups closely measure the sound excitation they would monitor at the internal surface, if physically feasible. The manhole chimney also was not reproduced because attachment of a mounting stud at positions 9, 10, and 12 would have been impractical.

Model positions 5 and 9 effectively substitute for the manhole vicinity sensor positions in the field. As shown by Fig. 7, the 60 inch (1.5 m) diameter concrete pipe was modeled by a 1/20th inch linear scale polyvinyl-chloride (PVC) plastic pipe which was cemented to the upstream face of the

thin wall concrete model turn section. Upstream of the attachement the supply pipe was configured to have the same geometric relationship (i.e., a 90 degree turn preceding the straight run) for the model as in the field. Not simulated, however, was the underground (buried) nature of the field installation. This was not done because the focus of the investigation was the 100 degree turn at the exit of the pipeline and not the pipeline itself.

Field site test data were limited to the single wet weather flow of 526 pps (3780 gpm) and dry weather flow (zero pps) conditions because of a prevailing (Spring) relatively low rainfall situation in the field test region during the normal work week; project budgeting made premium pay periods (e.g., weekends) unavailable for additional measurements during rainy episodes outside of scheduled work hours.

Sensor Position 4

Fourier Analyzer-processed sound data for this sensor mounting location, obtained with the laboratory scale model, are presented by Fig. 28 for eight different frequency band centers. These frequencies all represent cases of major sound intensities with clearly unambiguous signal variations with flow rate. The strongest trend is at a frequency of 480 Hz which corresponds to a wavelength of about 10 feet in water. There are no physical dimensions in the lab model, involving water flow, that are so large. Therefore, the source of the measured, apparently flow-related, sound is not presently determined. On the other hand, sound intensities at higher frequencies (e.g., 4000 and 6000 Hz) do also have usable signal-flow rate characteristics and do correspond to discontinuity dimensions that can be identified with the outfall channel enlargement of the laboratory model.

Sensor positions 3 and 5 on the headwall of the Cutter Mill Drain laboratory model bear superficial geometric similarity to position 4 on the Baldwin Creek model. However, a comparison of similarly processed sound data from these similar geometric positions on both models does not yield similar frequency or intensity trends. Therefore, the upstream channel

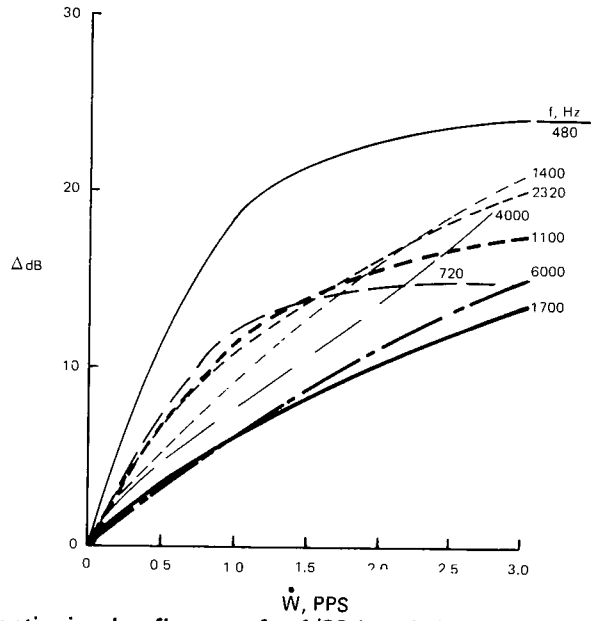

Figure 28. Acoustic signal vs flow rate for 1/20th scale laboratory model position 4 — Baldwin Creek field site geometry. Data processed by Fourier analyzer.

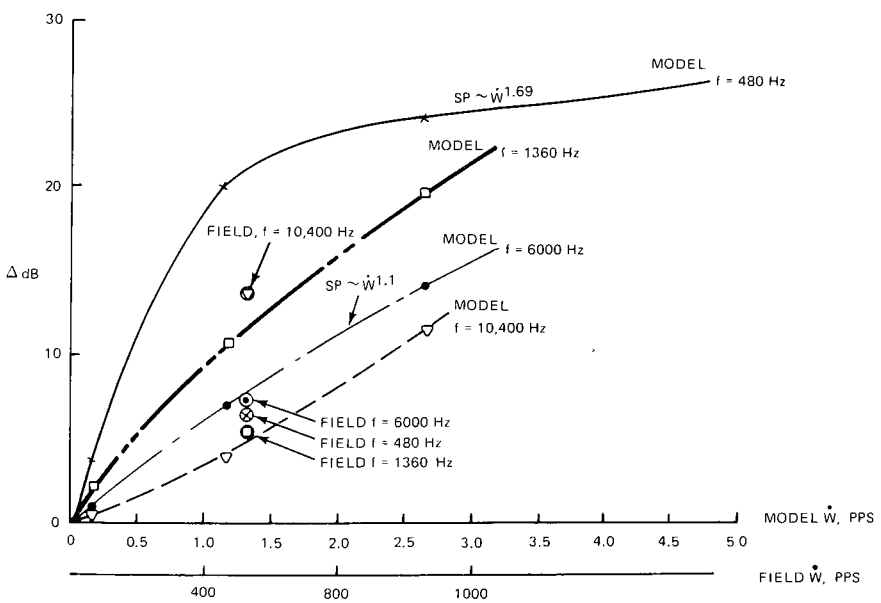

Figure 29. Comparison of laboratory and field data of acoustic signal vs flow rate at sensor position 4 - Baldwin Creek field site geometry. Data processed by Fourier analyzer.

differences of the two scale models obviously affect the exit flow profile of the outfall, and the sound emission characteristics.

The stormwater field data obtained at position 4 display a spectral distribution with a peak intensity at about 10,000 Hz. This frequency corresponds to a 6 inch (15 cm) dimension in water which can be approximately associated with the effects of a sudden increase in channel area, at the outfall, on the storwater flow level. Unfortunately, this hypothesis cannot be thoroughly tested because only one storm flow rate was documented. The laboratory scale tests provided no further insight into the sound source mechanism that was detected by the sensor at field position 4.

The Fourier-analyzed sound data obtained in the field and laboratory are compared in Fig. 29. It is evident that at any particular flow rate the lower range of frequencies have higher signal intensities for the model and approximately the opposite tendency for the field site. These trends, frankly, are counter to the expected behavior.

On the other hand, the comparable sound data from the GR 1933 monitor, shown by Fig. 30, is more in keeping with theoretical expectations. The model data measured by the GR 1933 meter at 480 Hz is about 3 dB below the field measurement if the associated respective flow rates are related by the flow area scale factor (i.e., 20 squared). The GR meter signal strength of the model measurements tend to decrease at higher frequencies (see Figs. 31a, b, c, and d), and the same trend is observed in the field. However, the field installation signals at the higher frequencies are of lower intensity than the model data for geometrically scaled similar flow rates. The GR 1933 monitor tends to miss fine detail of the sound spectra but detects the overall trend. Thus, the concurrence of the GR 1933 monitor's readings with general theoretical expectations seems to imply that the anomalous results obtained with the fine resolution Fourier processing probably are caused by inclusion of local resonances at the sensor position rather than by radically different physics. A more rigorous explanation would require a detailed sound survey to obtain direct and full casual relationships. However, because the primary objective of this investigation is to obtain field signals and sensor locations that can

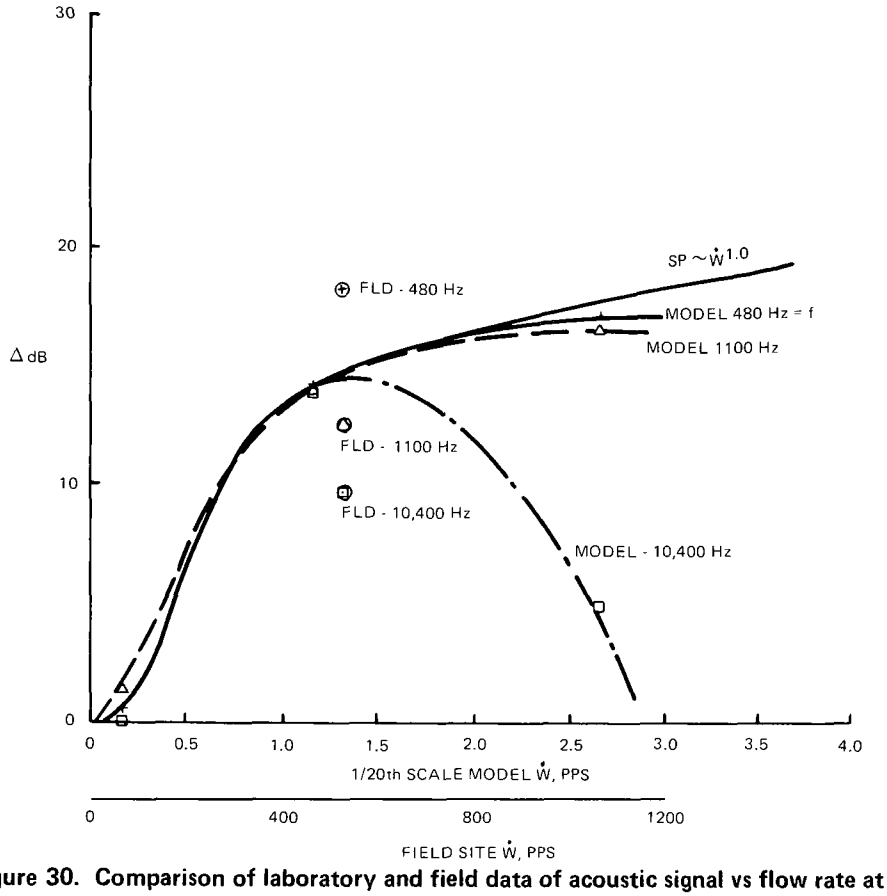

Figure 30. Comparison of laboratory and field data of acoustic signal vs flow rate at sensor position 4 - Baldwin Creek field site geometry. Data obtained by GR1933 Sound Meter with filter unit.

prove usable for flow measurements, we have succeeded in our quest without, frankly, being completely sure of the reason.

Spectral Distribution of Intensity

The comparative field intensity data for sensor positions 1, 4, and 7 shown by Fig. 32, indicate (through Fourier processing) that peak amplitudes are excited between 6000 and 11,000 Hz for these locations in the flow range encountered. Thus, the observations at position 4 seem more likely to have their origins in the flow distortion near the midpoint of the turn rather than with the end of the turn. This is another restatement of the principle that the most significant momentum loss affecting acoustic emission is where the flow vector changes the most. The single points spotted on

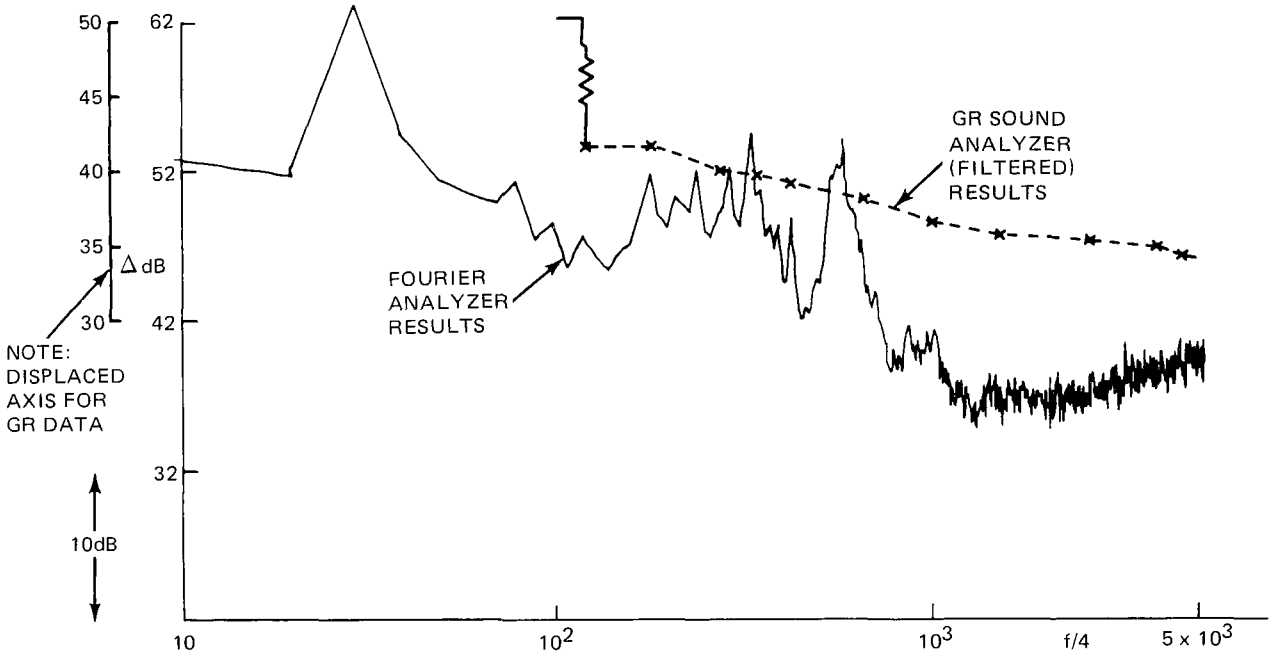

a. Zero flow rate (lab background noise).

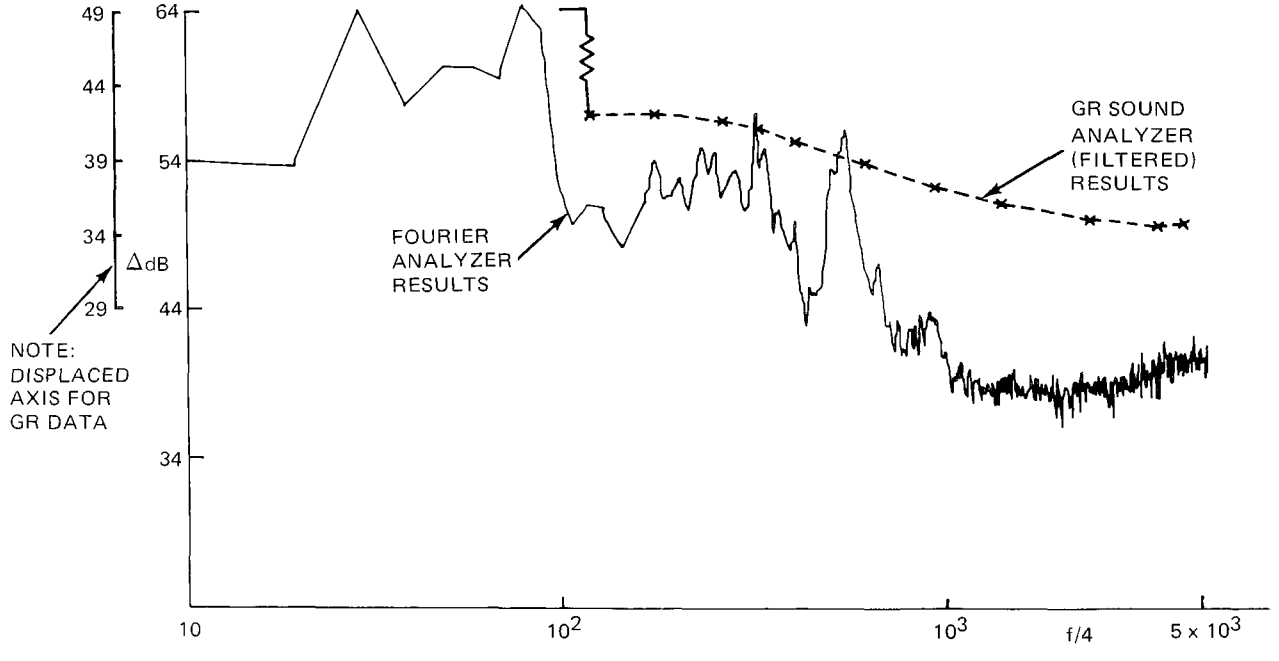

b. Flow rate of 0.175 pps.

Figure 31. Comparison of spectral distribution of intensity of acoustic emission signal obtained by General Radio 1933 Sound Meter vs. recorded data processed by Fourier Analyzer. Sensor position 4 on Baldwin Creek field site geometry model .

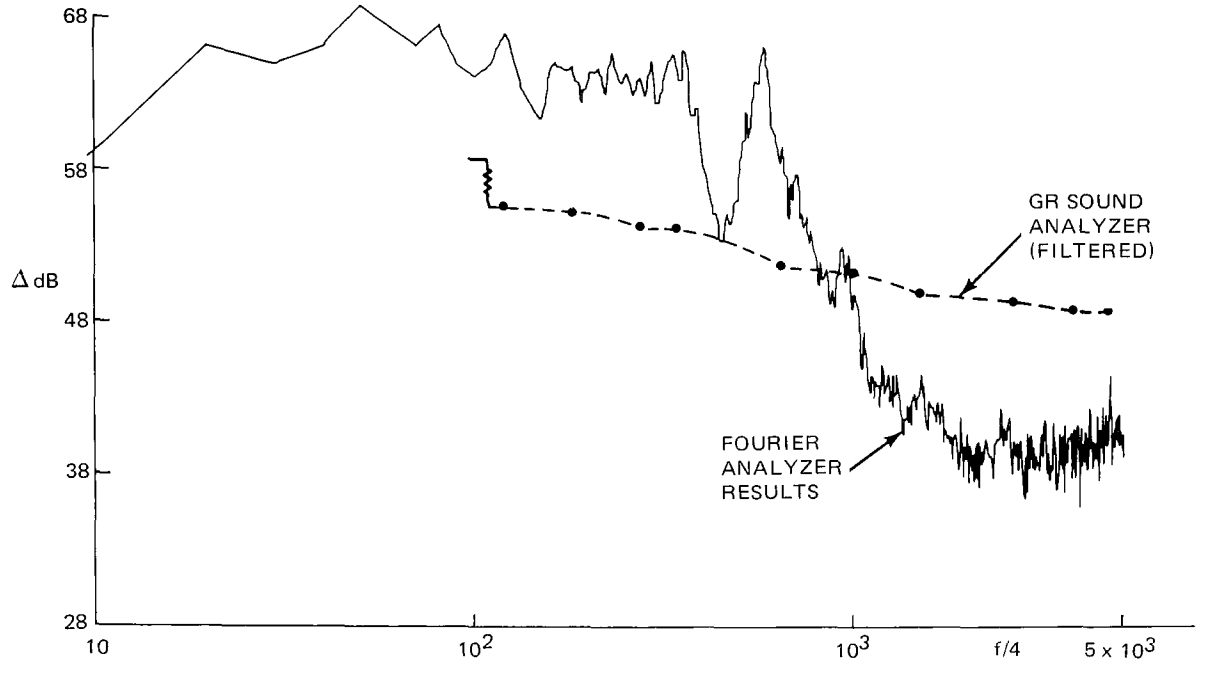

c. Flow rate of 1.15 PPS.

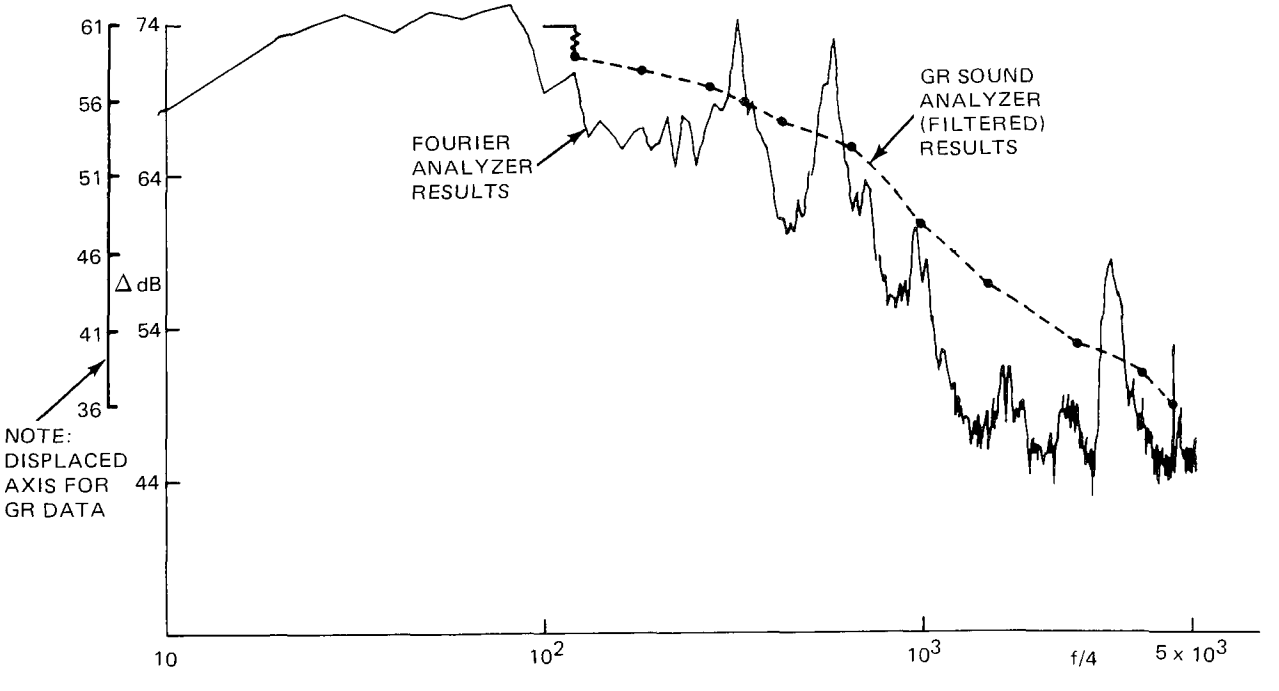

d. Flow rate of 2.65 PPS.

Figure 31. Comparison of spectral distribution of intensity of acoustic emission signal obtained by General Radio 1933 Sound Meter vs. recorded data processed by Fourier Analyzer. Sensor position 4 on Baldwin Creek field site geometry model

Fig. 32 for positions 5, 6, 8, 9 and 11 are the peak amplitudes in the 20-20,000 Hz range spectra at each position. Position 8 data reinforce the conclusion about the major source being at or near the midpoint of the turn, and the higher amplitude of position 8 compared to position 7 can be attributed to the former's closer proximity to the water flow. Position 11's relatively high signal at 8000 Hz may be associated with the abrupt channel cross sectional change at the beginning of the 100 degree turn section.

Some representative spectral distributions of the signals measured with the GR 1933 meter are shown by Fig. 33. In general, the filtered GR measurements obscure the fine features at the higher frequencies that are revealed with Fourier processing, as can be appreciated by reviewing Figs. 31a through d for the model tests. At the higher range of the frequency spectra, the intensity of the sound measured with the GR 1933 instrument appears

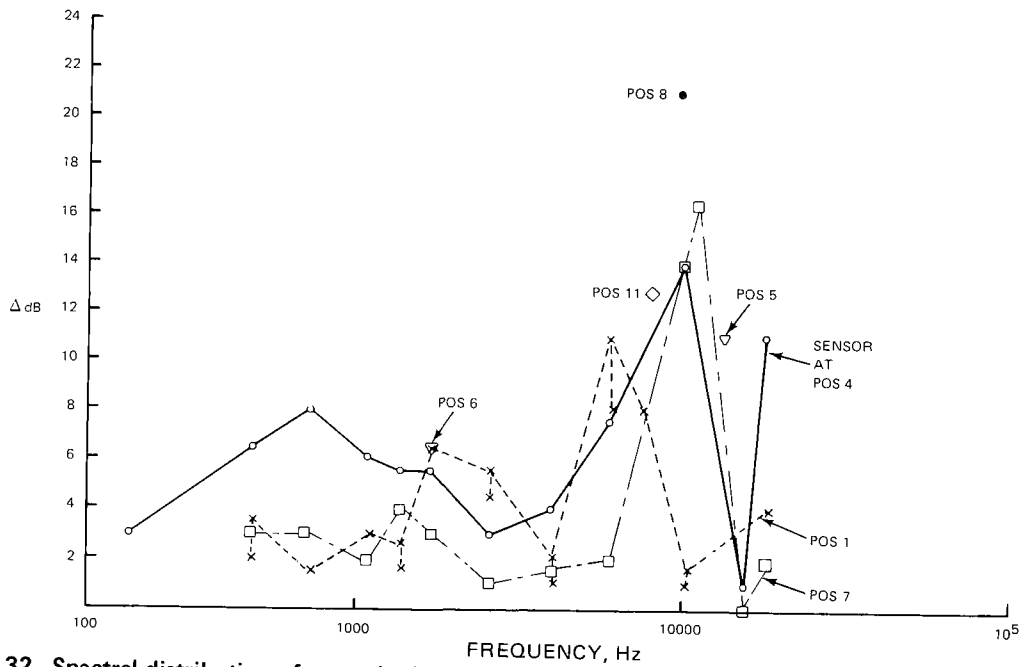

Figure 32. Spectral distribution of acoustic signal at several sensor positions of the Baldwin Creek field test site for a flow rate differential of 526 PPS. Recorded data processed by Fourier Analyzer

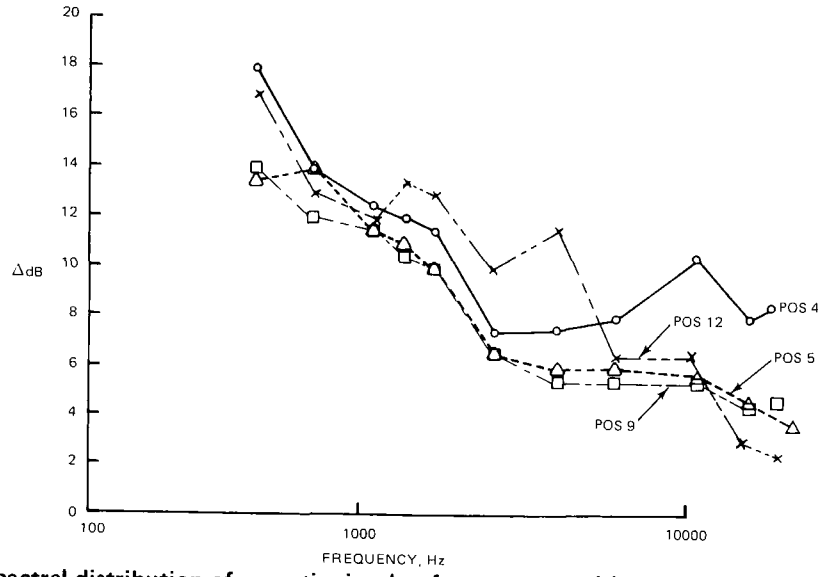

Figure 33. Spectral distribution of acoustic signal at four sensor positions of the Baldwin Creek field test site for a flow rate differential of 526 PPS. Data obtained by a GR1933 Sound Meter with filter unit.

higher than observed from Fourier processing. The apparent explanation for this is that the GR meter integrates the signal over a broader frequency band than the Fourier processing procedure normally includes. On a comparative basis, Fig. 33 indicates that the signal taken in the manhole chimney (position 12) is nearly as good in quality for flow measurement use as the outfall location (position 4). The signals immediately upstream or downstream of the manhole chimney (positions 9 and 5), but along the walls of the channel turn proper, are essentially equal and of somewhat lower intensity than in the manhole chimney itself. GR meter data at position 11 (not shown by Fig. 33) are similar to the position 9 signature, but are not quite as useful for our purposes, as by the full Fourier processed data method.

With the filtered GR 1933 meter, the lowest frequency (480 Hz) of peaking sound intensity, appears to give the best data agreement between field and model results at sensor position 9. With the theoretical mass flow scaling ratio used (i.e., 400), the field data of sound intensity at positions 4 and 7 are greater than the 1/20th scale model intensity results (see Fig. 34). However, a comparison at 480 Hz of model data results obtained by the Fourier analyzer and by direct GR 1933 readout processing techniques (Fig. 35) shows the two to be similarly unambiguous. However, the former gives greater intensity trends with flow rate. Therefore, the Fourier processed data has higher sensitivity for flow measurement purposes than the GR 1933 method with the Baldwin Creek geometry features. Furthermore, the frequency band center in which signal amplitude should be monitored is the best one (i.e., the one with peak signal intensity) which is

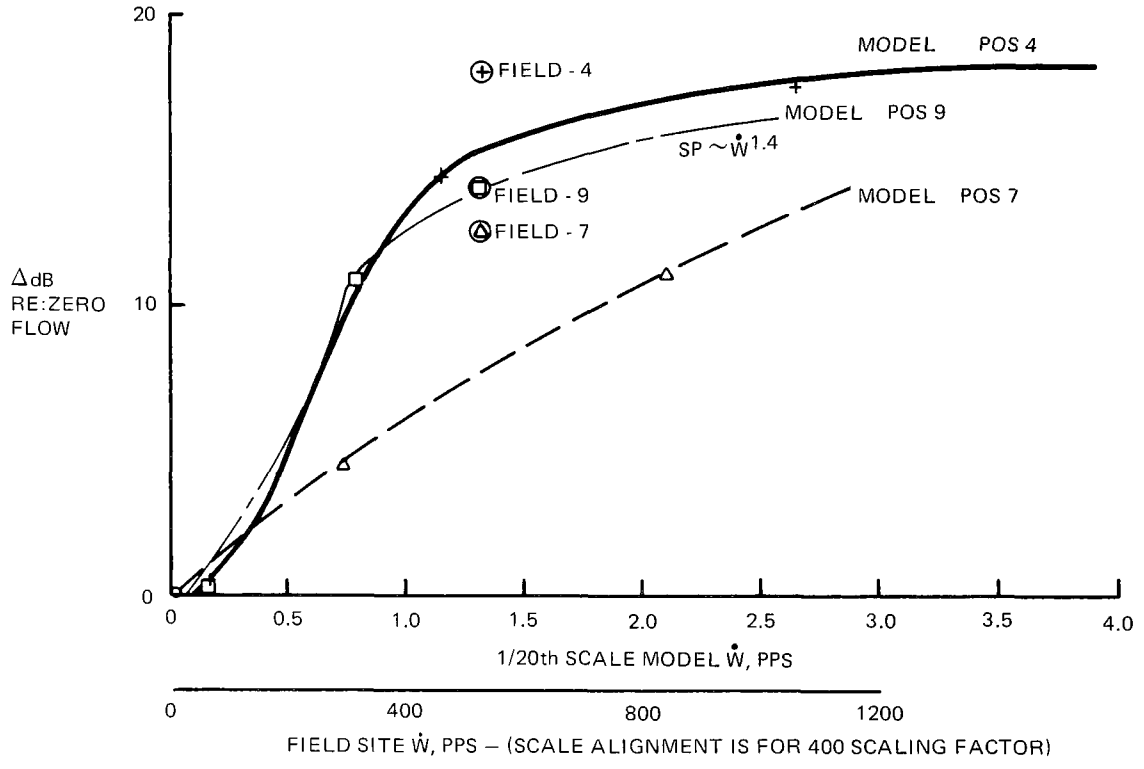

Figure 34. Comparison of field and laboratory data of acoustic signal vs flow rate at a frequency of 480 Hz. Three sensor installation positions of the Baldwin Creek field test site geometry. Data obtained by GR1933 Sound Meter with filter unit.

associated with the best measurement position and data processing technique (i.e., at position 4 the 10,400 Hz signal of the Fourier process rather than the 480 Hz signal of the GR 1933 process); compare Figs. 32 and 33.

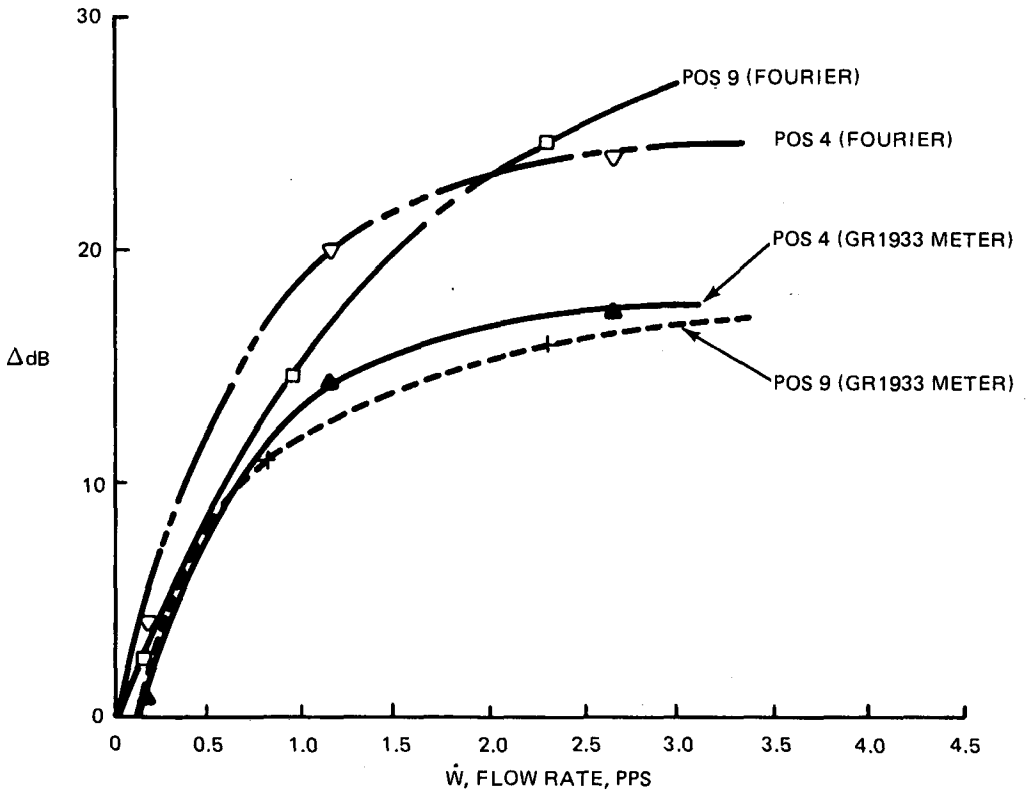

Figure 35. Comparison of measurement method on acoustic signal vs flow rate for two sensor installation positions on the laboratory model of the Baldwin Creek field test site geometry. Data at a frequency of 480 Hz.

SECTION 7

DISCUSSION

Because of the voluminous data obtained in the field and laboratory tests it is appropriate to place this investigation into perspective:

Notable from the viewpoint of the previous laboratory-bound investigation (Ref. 1) is the fact that the acoustic emission concept has been found to exist at three different field installations involving different channel discontinuities. The confirmation of the concept principle has been extended to flows that are two orders of magnitude greater than prior laboratory results (Ref. 1) and with real stormwater including Autumn-through-Summer seasonal changes of water quality. Sensor installations have been successfully deployed, without special safeguard, on public works structures for over ten months without being compromised by weather or human activity. Data were obtained in a manhole installation and found to provide usable signals for flow rate determination. The bulk of useful acoustic data were obtained with a prototype system that does not allow real time measurements. However, an approach was made toward an eventual compact, portable, real time, commercialized-type field apparatus utilizing a signal filtering unit and a rapidly responding sound meter. While the performance of the frequency filter interfered with a fully successful demonstration, especially for the upper portion of the audible frequency range (i.e., between 2000 and 20,000 Hz), the evidence is clear that such a system can work; elaborate Fourier processing facilities such as employed by the laboratory test and prototype instrumentation system are useful but not essentially for a flow measurement system based on flow acoustic emission at a channel discontinuity.

The field tests did reveal an aspect of large-dimensioned channels that was only partially appreciated beforehand. This involves the need to correct acoustic measurements for spatial radiation of the sound if the location of the sensor emplacement is distant from the apparent sound source.

However, such distance corrections are only required to adjust the signal of a single sensor monitoring low as well as high flow rates at an outfall. Biasing the sensor's installation location to the projection of one extreme rate of flow into the downstream channel requires a distance correction for the other flowrate extreme. This problem can be overcome by redundant sensors whose locations can bracket the full range of likely flows; sensor redundancy also improves system reliability. For manhole or channel directional change type discontinuity locations, there does not appear to be a need for a distance correction factor.

The use of scaled down, geometrically similar laboratory models to calibrate field installation was successful in being demonstrated. At certain select positions for sensor emplacement, there was good agreement of the signal intensity scaling law, using the geometric scale factor for mass flow correlation. The sound power was found related to flow rate to an exponent of between about 1.4 and 1.7, throughout the full flow rate range as indicated by Table 1. This power law relation translates into an increase of average sound intensity of 4 to 5 decibels for each doubling of flow rate. (The theoretical dipole relation for idealized, non-dissipative flow processes predicts a 12 decibel change for each doubling of flow rate.) Displaying the flow rate by a meter that is responsive to sound power, in absolute units, would give meter scale displacement ratios of 2.6 to 3.2 for each doubling of flow rate. However, the current theoretical expectations concerning the characteristic frequency band, at which the measurements were well correlated, were not encountered. There is a suspicion that this observation is associated with local resonances of the channel structure or sensor installation. Also, the relaxation of full dynamic similarity of the model flow may have contributed to this result. The prime focus of the current investigation precluded our following this question beyond the conjectures already raised. While our reasonably successful scaling demonstration without complete understanding of certain anomalies is uncomfortable, it is not without precedent for as new and unexplored a technology as we have employed in this innovative approach to sewer flow measurement. Further research, particularly to examine some unresolved questions such as revealed through this reported

investigation, has a high probability of indicating new and better ways to employ the full potential of the still largely unexploited flow acoustic emission principle.

TABLE 1 SELECTED MAJOR TEST RESULTS - ACOUSTIC EMISSION FLOWMETER

Channel Identification		Sensor Position	Band Center-Frequency Hz	Flow Rate Range, pps($\dot{w}$) Laboratory Model	Flow Rate Range, pps($\dot{w}$) Full Scale	Exponent "n" in SP ~ $\dot{w}^n$	Remarks Notes 1, 2
Cutter Mill Drain Lake Success, N.Y. area	Outfall	1	400	0-4.2	0-1680*	1.24	Lab data
			4000	0-4.2	0-1680*	0.62	Lab data
			1100		22-1040	1.60	Field site
			5600-7200		22-1040	1.15	Field site
			18000		22-230	1.20	Field site
	Wingwall	3	1050	0-4.2	0-1680*	1.89	Lab data
			2600	0-4.2	0-1680*	1.35	Lab data
			2900	0-4.2	0-1680*	1.95	Lab data 1 in. step
						1.20	Lab data ½ in. step
						1.0	Lab data no step
			18000		22-1040	0.95	Field-w/o sensor distance correction
						1.4	Field -w sensor distance correction
	Wingwall	5	2760	0-3.6	0-1440*	1.54	Lab data 1 in. step
	Check Dam	20	960	0-5.1	0-2040*	2.2	Lab data
			1400	0-5.1	0-2040*	2.5	Lab data
			1920	0-5.1	0-2040*	2.9	Lab data
			3800	0-5.1	0-2040*	1.9	Lab data
			3800		22-1040	1.09	Field-w/o sensor distance correction
			3800		22-1040	1.6	Field-w sensor distance correction
Baldwin Creek Baldwin, N.Y. area	Outfall - (downstream of 100 degree turn section)	4	480	0.1-2.65	40-1060*	1.0	Lab data - General Radio 1933 Sound Meter + Filter
			1100	0.1-2.65	40-1060*	1.0	
			480	0.1-2.65	40-1060*	1.69	Lab data
			6000	0.1-2.65	40-1060*	1.1	Lab data
					0-526	1.1	Field data - coincides with Lab data
	Base of manhole chimney in 100 degree turn section	9	480	0.1-2.3	40-920*	1.4	Lab data - General Radio 1933 Sound Meter + Filter
					0-526	1.4	Field data - coincides with Lab data
			480	0.15-2.3	60-920*	1.85	Lab data
	Midway in turn of 100 degree turn section	5	480	0.15-2.9	60-1160*	1.69	Lab data

Notes 1 All data processed by Fourier Analyzer unless otherwise noted.
2 All laboratory data with 1/20th scale models.

* Equivalent full scale flows applying 400 x scaling factor.

REFERENCES

1. Foreman, K.M. A Passive Flow Measurement System for Storm and Combined Sewers. EPA-600/2-76-115, U.S. Environmental Protection Agency, Cincinnati, Ohio, May, 1976. 123 pp.

2. Ffowcs-Williams, J. Hydrodynamic Noise. In: Annual Reviews of Fluid Mechanics. Vol. 1 Annual Reviews, Inc. Palo Alto, CA, 1969.

3. Blokhintsev, D.I. Acoustics of a Non-Homogeneous Moving Medium. NACA TM 1399, National Advisory Committee for Aeronautics, Washington, D.C. February 1956.

4. Ver, I.L. and C.I. Holmer. Interaction of Sound Waves with Solid Surfaces. In: Noise and Vibration Control, L.L. Beranek, ed., McGraw-Hill Book Co., New York, N.Y., 1971. pp. 270-361.

GLOSSARY

accelerometer: An electromechanical transducer that generates an electrical output when subjected to acceleration. Piezoelectric discs clamped between a mass and base develop a potential field when the acceleration of the mass exerts a force on the discs. The ratio of electrical output to mechanical input is called sensitivity.

acoustic emission: The radiation of sound generated by the interaction of fluid flow with a solid surface.

acoustic reflection: The change of direction of sound pressure waves impinging on a less than perfect sound absorbing surface.

conduit discontinuity: Any change in a flow channel because of channel cross section or shape, or where flow direction is significantly changed.

decibels (dB): A measure of the ratio of two amounts of sound power. The range of sound pressure or intensity is so large that it is more convenient to use the logarithm to the base ten to express this ratio (bel). Decibel equals one tenth of a bel. When other quantities (e.g., voltage) are related to the square root of power, the number, n, of dB are: $n = 20 \log_{10}(v/v_o)$, where v_o is the referenced quantity.

dipole: The type of sound source created when a fluid interacts with a solid surface to produce unsteady forces. Because of its oscillating nature, this source is analogous to two point-sources equal in strength but opposite in phase and separated by a very small distance. The radiated power is proportional to the fourth power of flow speed. Because of the pressure cancellation in the plane normal to the dipole axis, the directionality of radiation is strongest along the dipole axis which is normal to the flow direction.

hertz (Hz): An international unit of frequency equal to the number of cycles per second.

nonintrusive: Not penetrating the fluid flow boundary.

normalized acoustic signal: When transducers of different sensitivities measure the same sound source, their dB sound signals are different by the ratio of sensitivities. Similarly, when a constant sound source signal is measured against different background noise levels, the total signals are different by the relative difference in backgrounds. When using decibel units for sound level, the irrelevant variables of measurement such as background noise or sensor sensitivity can be eliminated by subtracting their dB contribution from the total signal. The resulting dB level then is the normalized signal, and is a more valid measure of the sound source alone.

overburden: The soil or backfill covering a buried sewer pipe or flow conduit.

passive flow measurement: A method of determining the mass or volumetric rate of flow by using energy normally radiated by the fluid flow as opposed to imposing external energy sources or flow energy dissipating devices.

pseudosound: The pressure pulses produced in locally disturbed fluid flow that have characteristics of sound in the near field but do not propagate into the far field of the fluid. The radiation pattern of pseudosound is like a dipole sound source.

sound power (SP_T): The total amount of energy radiated by a sound source throughout a spherical envelope in a period of time (watts). In practice, the sound power level, L_w, is used to relate the ratio of sound power to a reference power. By international agreement, this reference power is 10^{-12} watts, and $L_w = 10 \log_{10}(P_T/10^{-12})$, dB.

unambiguous signal: A sensor output signal that can be interpreted as relating to only one flow quantity. Over a continuous range of signal output there are no intermediate minima or maxima with regard to the dependent parameter.

TECHNICAL REPORT DATA
(Please read Instructions on the reverse before completing)

1. REPORT NO.	2.	3. RECIPIENT'S ACCESSION NO.
EPA-600/2-79-084		

4. TITLE AND SUBTITLE
Field Testing of Prototype Acoustic Emission Sewer Flowmeter

5. REPORT DATE
August 1979 (Issuing Date)

6. PERFORMING ORGANIZATION CODE

7. AUTHOR(S)
K.M. Foreman

8. PERFORMING ORGANIZATION REPORT NO.
RE- 566

9. PERFORMING ORGANIZATION NAME AND ADDRESS
Research Department
Grumman Aerospace Corporation
Bethpage, New York 11714

10. PROGRAM ELEMENT NO.
1BC822, SOS 1, Task 47

11. CONTRACT/GRANT NO.
EPA Contract 68-03-2525

12. SPONSORING AGENCY NAME AND ADDRESS
Municipal Environmental Research Laboratory--Cin.,OH
Office of Research and Development
U.S. Environmental Protection Agency
Cincinnati, Ohio 45268

13. TYPE OF REPORT AND PERIOD COVERED
Final Report 7/6/77-10/6/78

14. SPONSORING AGENCY CODE
EPA/600/14

15. SUPPLEMENTARY NOTES See also EPA-600/2-76-115, "A Passive Flow Measurement System for Storm and Combined Sewers"
PO: Hugh Masters, (201) 321-6678, (8-340-6678)

16. ABSTRACT

This investigation concerns verifying the operating principles of the acoustic emission flowmeter (U.S. Patent 3,958,458) in the natural environment of three different storm sewer field sites in Nassau County, New York. The flowmeter is a novel, passive, nonintrusive method that uses the local sound resulting from the partial transformation of the flow energy at a channel or conduit discontinuity. Any change of sewer cross section or flow direction qualifies as a discontinuity.

The results show that the flowmeter principles hold true in large storm sewers of 60 inch (1.5 m) diameter and for flow rates up to about 7500 gpm. A manhole appears to be suitable for sensor installation. The relation of sound signal intensity to flow rate at full scale sites appears amenable to small scale laborabory model simulation according to scaling laws.

Recommendations are offered for future testing and design activities.

17. KEY WORDS AND DOCUMENT ANALYSIS

a. DESCRIPTORS	b. IDENTIFIERS/OPEN ENDED TERMS	c. COSATI Field/Group
Flow, Acoustics, Sewers, Flowmeters, Experimental design, Acoustic signatures, Sound level meters	Acoustic emission, Flowmeter	20C, 20A 13B 14B 17A 9A, 9B

18. DISTRIBUTION STATEMENT	19. SECURITY CLASS *(This Report)*	21. NO. OF PAGES
RELEASE TO PUBLIC	Unclassified	79
	20. SECURITY CLASS *(This page)* Unclassified	22. PRICE

☆ U S GOVERNMENT PRINTING OFFICE: 1979 -657-146/5465